MASTER'S THESIS

Analysis of Microfibrillated Cellulose (MFC) in a shotcrete mix-design

– An investigation on the physical, mechanical, and rheological properties

Farhan Khalique Awan

August 15, 2023

Author Farhan Khalique Awan

Title of thesis Analysis of Microfibrillated Cellulose (MFC) in a shotcrete mix-design – An investigation on the physical, mechanical, and rheological properties

Programme Master's Programme in Green Energy Technology

Major Materials in Energy Technology

Thesis internal supervisor Dr. Shima Pilehvar

Thesis external advisor Dr. Harrison Gallantree-Smith

Collaborative partners Borregaard, Østfold University College

Date 15.08.2023   **Number of pages** 86   **Language** English

Declaration

I, Farhan Khalique Awan, declare that the contents of this dissertation reflect solely my independent effort, and it has not been previously presented for any academic assessment. It reflects my personal views, not necessarily those of Østfold University College.

August 15, 2023

Farhan Khalique Awan   Date

Acknowledgement

I would like to express my heartfelt gratitude to all those who have supported me throughout my journey in completing this master's thesis. Their unwavering encouragement, guidance, and assistance have been invaluable to me.

First and foremost, I extend my deepest appreciation to my thesis internal supervisor, Associate Prof. Shima Pilehvar, and Dr. Harrison Smith, for their expertise, guidance, and insightful feedback. Their dedication to my project and willingness to share their knowledge have been instrumental in shaping the direction of my research.

I would also like to thank Professor Anna-Lena Kjøniksen for inspiring me towards research, and Associate Prof. Susana Garcia for training me in several laboratory instruments and data analysis. I would also like to thank PhD re-searcher Parham Shoei for his help and support in the laboratory.

I wish to express my gratitude to Østfold University College for creating an environment conducive to both learning and personal development. The department's provided resources and facilities have played a vital role in facilitating the effective progression of my research.

To my circle of friends, colleagues, your camaraderie, and discussions have helped me refine my ideas and maintain my motivation.

Last, but not the least, I am grateful to my family for their unwavering support, both emotionally and morally, throughout this journey. Their constant belief in my abilities has been my driving force.

In conclusion, completing this thesis has been a challenging yet rewarding experience, and I am grateful to all those who have played a role, big or small, in its realization.

Thank you.

Contents

Summary

Shotcrete, widely used in construction, has proven valuable in tunneling and mining due to its adaptability and historical significance. However, its environmental impact and property challenges have prompted innovative solutions. Promotion of sustainability in the construction industry, particularly shotcrete production entails strategies like replacing cement with low-carbon alternatives or improving the plastic yield stress of fresh shotcrete, crucial for controlling rebound and maximum build-up thickness without altering the water-to-cement ratio. Recently, Microfibrillated Cellulose (MFC), derived from the Norwegian Spruce in abundance all over Scandinavia has emerged as a compelling option in the shotcrete field, offering improved sustainability and cost-effectiveness. MFC's rheological effects encompass shear thinning behavior, potentially enhancing shotcrete stiffness post-application and base mix stability.

This research delves into a preliminary investigation of MFC's advantages in shotcrete through a series of laboratory tests focused on the determination physical, mechanical, rheological and chemical properties and comparison with a base control sample as reference. The primary focus was to assess MFC's impact on rebound potential, as well as its workability, compressive and flexural strength, rheology, and hydration kinetics.

Results indicate that MFC acts as a Viscosity-Modifying Admixture (VMA), while maintaining suitable workability and pumpability, suggesting potential for reduced rebound. The inclusion of MFC results in improving the mechanical strength of the shotcrete mix, however, this effect is within a range of dosage. Importantly, MFC doesn't disrupt shotcrete mix hydration kinetics, showcasing its compatibility. This study highlights MFC's potential in enhancing shotcrete properties while aligning with sustainable construction practices and environmental consciousness.

Keywords: Microfibrillated Cellulose, shotcrete, admixtures, sustainability, carbon-footprint

Thesis structure

This thesis is divided in 9 chapters. **Chapter 1** introduces the shotcrete industry, its advantage over conventional concrete, and highlights the environmental impacts posed by the usage of cement in the construction industry. It also discusses the problem of excessive usage of cement and various methods to mitigate its usage, including the role of Microfibrillated Cellulose (MFC) being successful in concrete designs.

Chapter 2 provides a background in associated literature, pertaining to shotcrete preparation, effects of different additives and admixtures, and understanding parameters for shotcrete performance measurement.

Chapter 3 is focused on defining the aim of this thesis, which serves its direction and scope.

Chapter 4 gives an insight into the methodology utilized in this research, with a detailed characterization of the raw materials used, experimental design and testing methods that are employed.

Chapter 5 showcases the experimental results pertaining to the physical and mechanical properties of all the shotcrete mix designs.

Chapter 6 highlights the experimental results pertaining to the flow properties (rheology) and chemical properties (heat of hydration) of all the shotcrete paste mix-designs.

Chapter 7 is focused on a discussion over the obtained results and outcomes.

Chapter 8 concludes the research work focusing on the most important outcomes with their implication.

Chapter 9 discusses the future potential and expansion of this research.

Table of figures

List of tables

1   Introduction

Shotcrete, also known as spray-applied concrete, is a commonly used construction material that has gained widespread popularity in the construction industry, especially tunnelling and mining sectors. Its use in rock reinforcement and other civil construction applications dates back to the 1930s, making it a well-established technique with a long history of utilization in these industries [1]. Its versatility lies in its easy application, adherence to various shapes, as well as bonding on uneven surfaces [2]. Over the years, the credibility of shotcrete as a viable construction technique can be attributed to the introduction of cutting-edge technologies such as Supplementary Cementitious Materials (SCMs), advanced chemical admixtures as well as fiber reinforcement [3]. However, this is marred by its significant environmental impact, which is around 5% of the atmospheric CO_2 emissions on a global scale [4]. This problem has been addressed in several ways including (1) addition of low-carbon footprint induced SCMs in cement production, (2) decreasing usage of cement by utilizing higher water-to-cement ratio via different additives and admixtures, and (3) developing optimum shotcrete mix-design depending on application to improve rebound and built-up thickness [5] [6].

Following the trend of reducing environmental impact, there have been increasing studies on the utilization of Microfibrillated Cellulose (MFC) as a bio-additive in concrete with positive results as it has been found to have a rheology modifying effect on mortar and concrete mixtures, on properties like shear thinning behaviour and high zero-shear viscosity. This research can be pursued in shotcrete designs as well since MFC exhibit potential improvement in immediate stiffness, workability, and stability of concrete without altering water-to-cement ratio (w/c). From a sustainability perspective, utilization of MFC can reduce cementitious material in the mix-design with possible improvement in cost-efficiency with fresh-state performance, as well as significantly low carbon footprint due to the bio-based nature of MFC [7].

This report is focused on researching the impact of Microfibrillated Cellulose (MFC) in shotcrete mix-design. The benefits of using MFC in shotcrete need to be supported via standardized laboratory tests and validation. There should also be compatibility between MFC the other additives in the mix design. The overall performance of shotcrete (mechanical strength and workability) should also not be adversely affected.

2   Literature review

2.1   Shotcrete

Shotcrete, also commonly known as sprayed concrete or gunite, is a type of composite material applied via spraying a mixture of cement, aggregates, and additives or admixtures at high a velocity onto the desired surface. It is commonly utilized in applications that are limited by the traditional concrete placement methods, such as uneven surfaces, repair work, slope stabilization, and tunnelling being the most popular area of usage [8]. The basic ingredients for shotcrete preparation include the following: (1) Cement, as a binding material, (2) Aggregate, to provide bulk and volume to the shotcrete mix and contribute to overall strength and density, (3) Water, for the hydration process of cement, as well as workability and strength, and (4) Admixture, to modify shotcrete properties such as setting times, mechanical strength and rheology [9].

2.2   Methods of shotcrete preparation

2.2.1   Dry-mix process

In the dry-mix process, Binders and aggregates are dry mixed and fed into a delivery hose. The mix is delivered via pneumatic pressure to the nozzle, with the addition of pressurized water. This water is uniformly injected into the mixture as it is discharged from the nozzle and propelled against the receiving surface [10]. This is illustrated in figure (1).
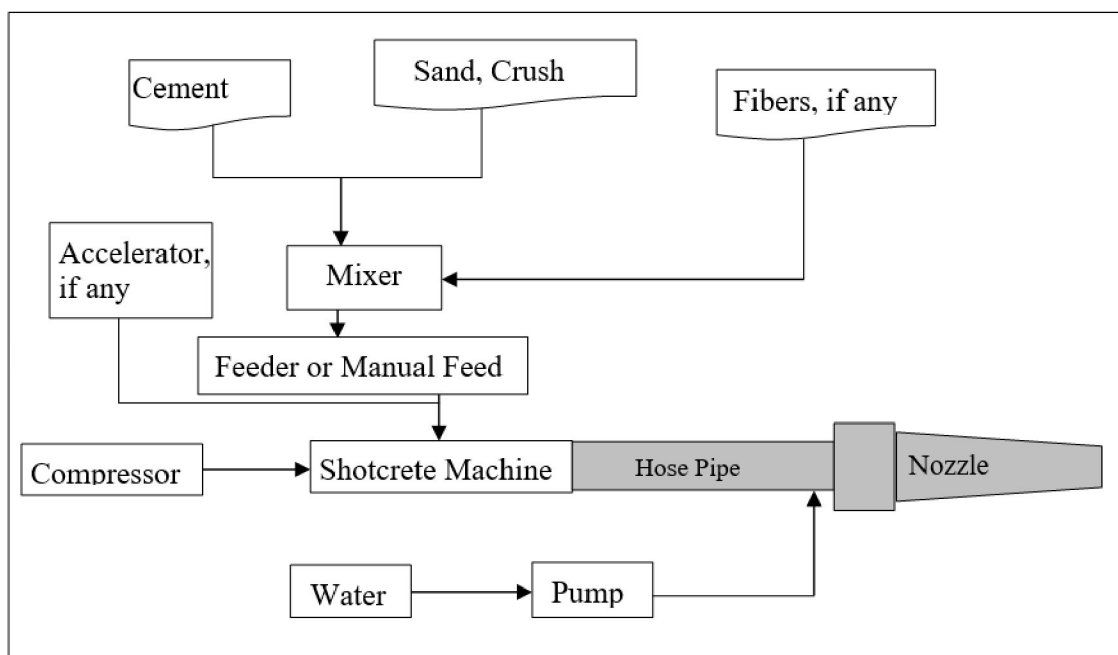
Figure 1. Shotcrete dry-mix process schematic [11].

2.2.2   Wet-mix process

In the wet-mix process, cement, aggregates, water, and admixtures are all mixed (just like conventional concrete). The mix is then fed to a concrete pump. This pump delivers the mixture through the delivery hose, [10] as shown in fig. (2).
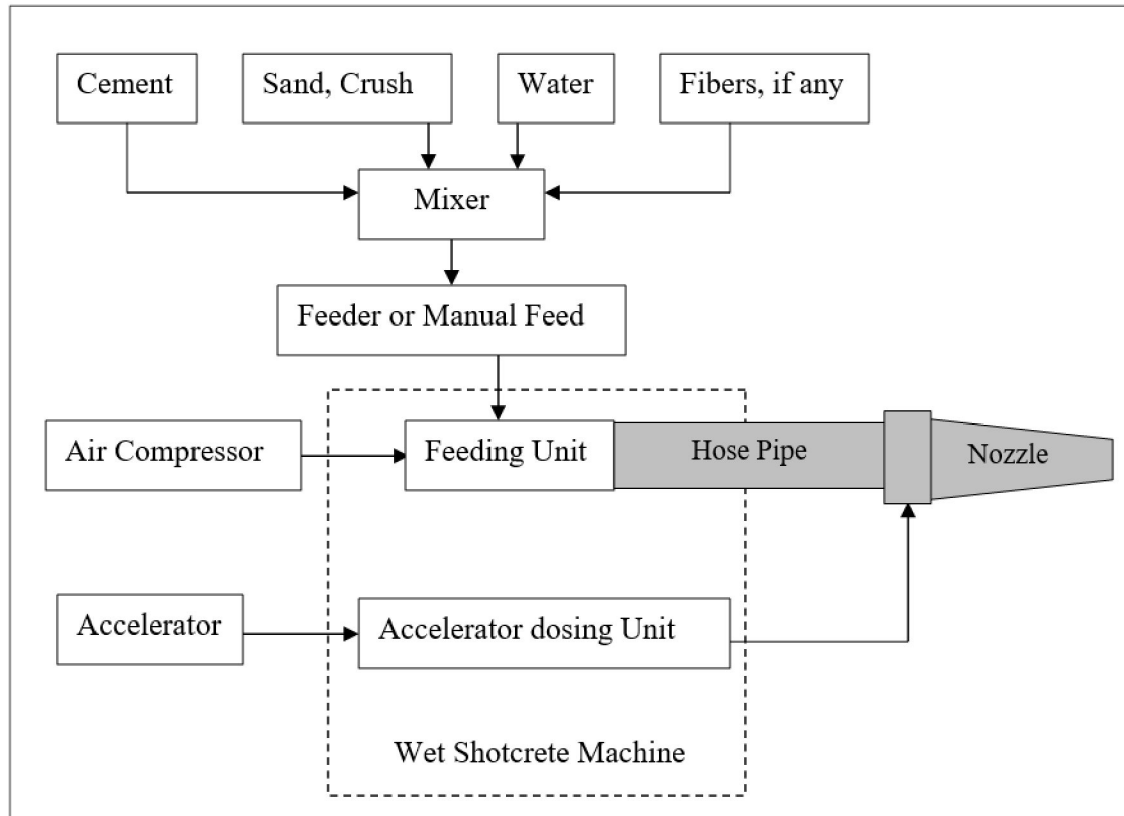
Figure 2. Shotcrete wet-mix process schematic [11].

2.2.3   Comparison between the dry-mix and wet-mix process

The key differences between dry-mix and wet-mix are summarized in table (1).

Table 1. Comparison between dry and wet-mix shotcrete procedure [11]

Dry-mix process	Wet-mix process
Operator can instantaneously control the mixing water at the nozzle to meet variable field conditions.	Moving water controlled at plant and measured at the time of batching.
Longer hose lengths possible.	Normal pumping distances necessary.
Limited to accelerators as the only practical admixture.	Compatible with all ordinary admixtures.

Resistance to freezing and thawing is poor.	Acceptable resistance to freezing and thawing.
Intermittent use easily accommodated within prescribed time limits.	Best suited in case of continuous shotcrete application.
Exceptional strength performance possible.	Lower strengths, similar to conventional concrete.
Lower production rates.	Higher production rate.
Higher rebound.	Lower rebound.
Lower equipment maintenance costs.	Higher equipment maintenance costs.
Higher bond strengths.	Lower bond strengths (higher than conventional concrete).

This research is focused on preparation of different shotcrete samples via wet-mix process, based on the following reasons: (1) lower rebound rate and dust, which is an essential criteria and topic of focus in shotcrete research, (2) possibility of higher production rate and continuous operation, and (3) compatibility with all admixtures [12].

2.3   Admixtures

Admixtures are specialized additives incorporated into the shotcrete mix for enhancement of its properties and performance in fresh and hardened state. They can provide several benefits including improved workability, accelerated setting times, enhanced durability, reduced shrinkage, and better adhesion to surfaces [13]. Utilization of admixtures can also help control the amount of cementitious material used in shotcrete or concrete production, which contributes to sustainable construction practices. The chemistry of admixtures (synthetic and bio-based), in conjunction with the mixing water, play an important role in elevating shotcrete mixes to the design-mix having high performance [9].

2.3.1   Impact of admixtures on the rheological properties of wet-mix shotcrete

Different additives and admixtures are included in shotcrete for improving its strength, adhesion, cohesion, resistance to freezing/thawing and abrasion, and to decrease rebound. These enhancements are applicable to both dry and wet processes. In dry-mix process, these additives elevate initial strength, decrease dust and rebound, whereas in wet-mix

design, they aid in achieving swift setting and early strength development, and decrease rebound compared to reference samples [9].

Yun et al. [14] conducted a study to investigate the impact of various admixtures on the rheological characteristics of high-performance wet-mix shotcrete (HPWMS), with the objective to tackle practical difficulties encountered during the conventional processing of wet-mix shotcrete. This study was carried out with the following tests (1) Air content test (pressure method), (2) Rheological test (IBB rheometer), with focus on flow resistance, torque viscosity [14]. Table (2) shows the admixtures utilized in this study.

Table 2. Experimental admixtures [14].

Variables	Target levels
w/c	0.50, 0.55, 0.60
AEA (% of cement content)	0, 0.01, 0.02, 0.05
Superplasticizer (% of cement content)	0, 0.1, 0.2
Silica fume (% of cement content)	0, 9
Polymer (% of cement content)	0, 0.2
Synthetic fiber (% of cement content)	0, 0.2
Viscosity agent (% of cement content)	0, 0.3

The study outcomes indicated that the incorporation of an air-entraining admixture (AEA) led to a corresponding decrease in flow resistance and torque viscosity in High Performance Wet-Mix Shotcrete (HPWMS). In contrast, the influence of the superplasticizer predominantly affected flow resistance, whereas its impact on torque viscosity was comparatively less pronounced. Furthermore, the introduction of silica fume resulted in a substantial rise in flow resistance, coupled with a minor reduction in torque viscosity. This pattern suggests that silica fume is highly effective in enhancing the rheological attributes of shotcrete, particularly in terms of improving its shootability and pumpability [14]. Results from these experiments are illustrated in fig (3), (4), (5), (6), (7), and (8).

(a)   (b)
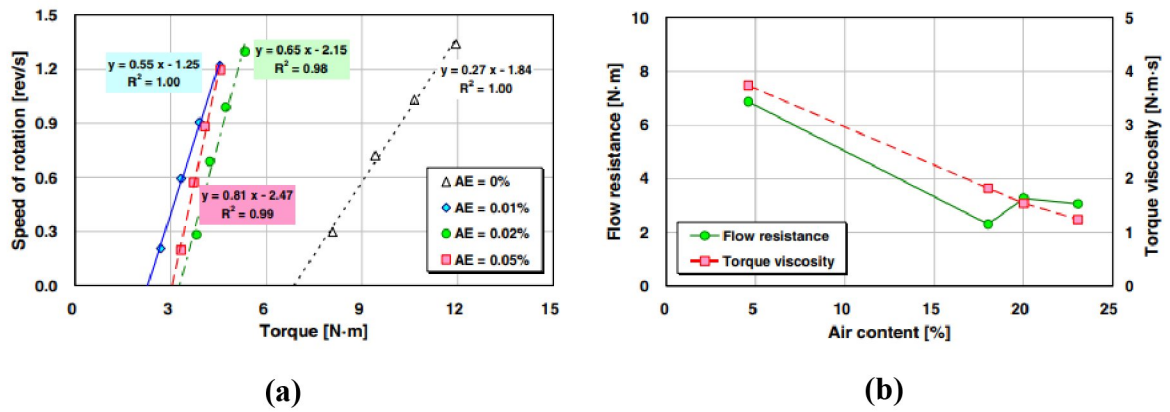
Figure 3. Impact of Air Entraining Admixture on (a) Torque, and (b) flow resistance [14]

(a)   (b)
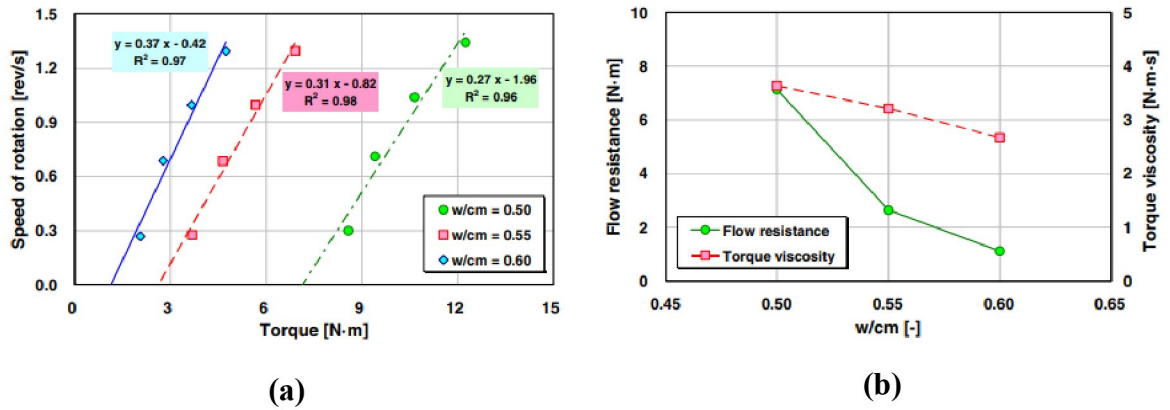
Figure 4. Impact of w/cm on (a) Torque, and (b) flow resistance [14]

(a)   (b)
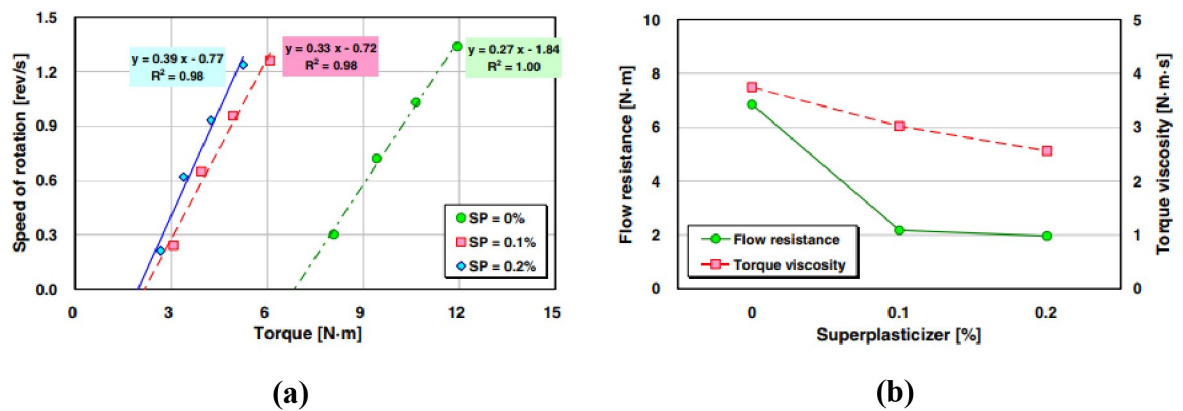
Figure 5. Effect of superplasticizer on (a) Torque, (b) flow resistance [14]
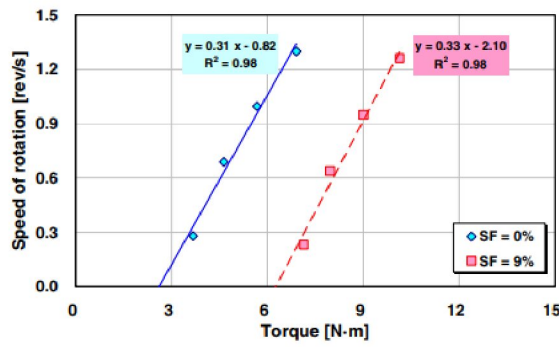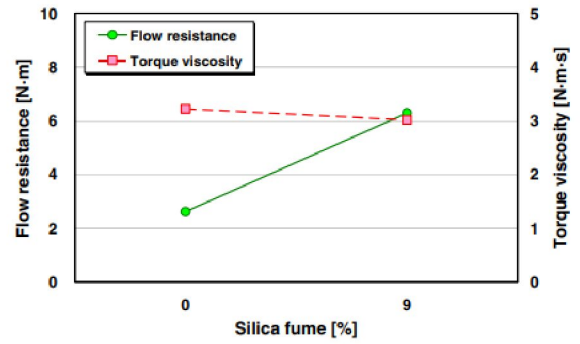
Figure 6. Effect of superplasticizer on (a) Torque, (b) flow resistance [14]
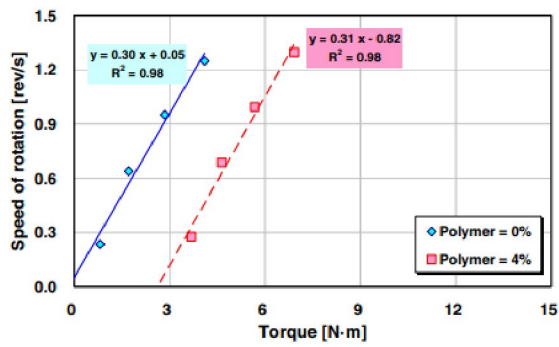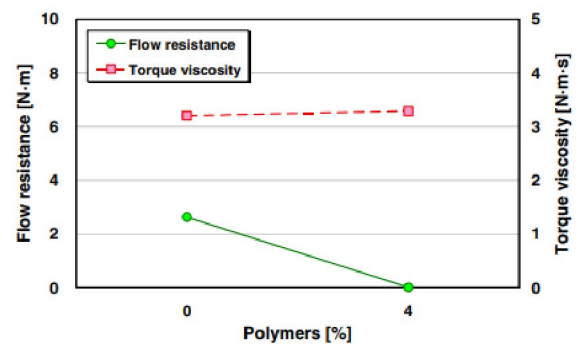
Figure 7. Effect of polymer on (a) Torque, (b) flow resistance [14]
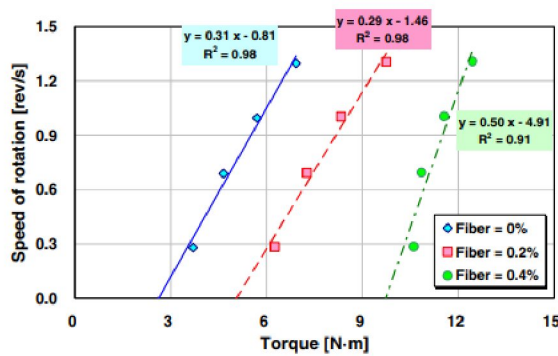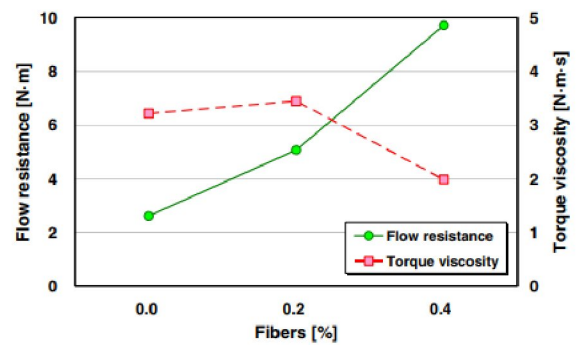
Figure 8. Effect of synthetic fibers on (a) Torque, (b) flow resistance [14]

2.4   Shotcrete performance measures

Shotcrete performance is assessed using a range of measures to ensure its suitability for construction applications and its durability over time. These measures are derived from both its fresh and hardened or cured state. Study into these properties and performance opportunities provide an insight into future enhancement using Microfibrillated Cellulose (MFC) admixture.

2.4.1   Fresh state performance measurement

In its fresh state, shotcrete rheology defines its performance in terms of rebound. The relationship between rheological parameters and the rebound of shotcrete is demonstrated through properties like slump, yield stress, plastic viscosity, air-content and the bleeding rate of fresh shotcrete. These characteristics comprehensively affect the rheological attributes like workability, pumpability, adhesion, sprayability, and rebound behavior [15].

2.4.1.1 Shotcrete rebound

Rebounding refers to the amount of shotcrete that is unable to adhere to the surface during its application, affecting both cost-efficiency and time needed for spraying. It can have significant impacts on cost-efficiency and required spraying time. In the wet-mix approach, rebound usually falls within 5-15% of the applied shotcrete, whereas the dry-mix technique may yield higher rebound levels of approximately 20-30% [6].

Shotcrete rebound can be divided into three components: (1) cement slurry, (2) fine aggregates, and (3) coarse aggregate part. Fig. (9) illustrates the rebound effect of a shotcrete mix, while its material distribution in the vertical section is depicted in fig. (10), showcasing the rebound distance of the three components [15].
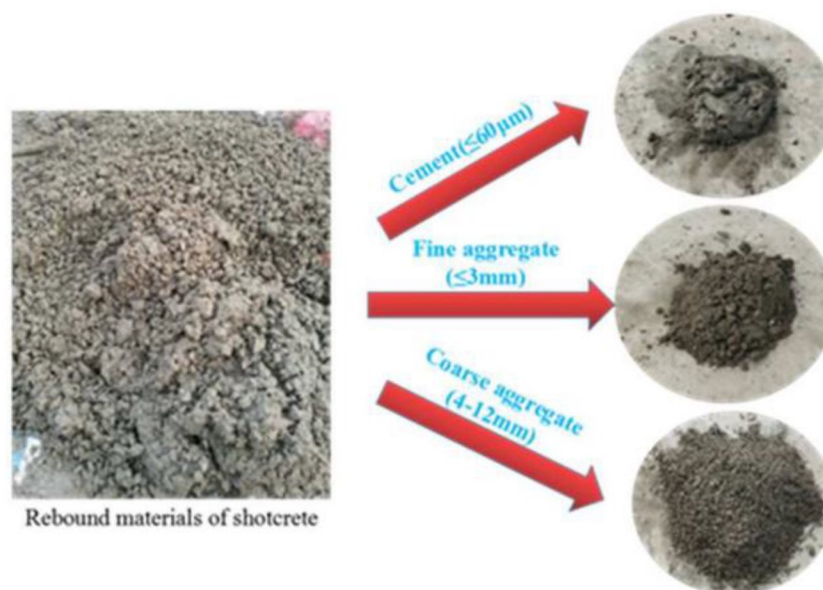
Figure 9. Shotcrete material division in rebound [15]
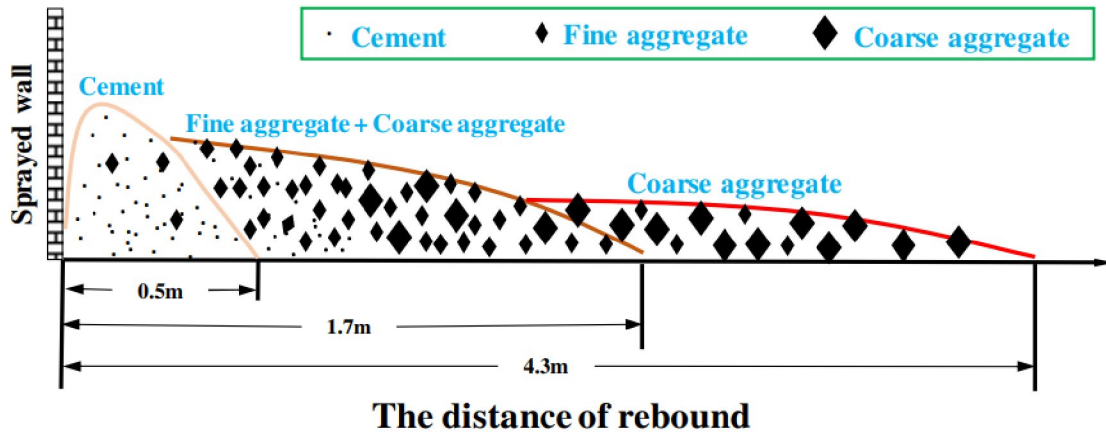
Figure 10. Rebound material distribution from vertical wall [15].

Rebound rate is calculated as the percentage of material lost during spraying, as following:

$$R = \frac{m}{M} \times 100$$

Where, R is the rebound rate (%), m is the mass of material lost as rebound (kg), and M is the total mass of material sprayed (kg) [15].

According to established research, various factors affecting the application performance of freshly sprayed shotcrete (such as slump, air content, and bleeding rate), show a direct correlation with rebound volume in the wet-mix shotcrete method [16]. This indicates that higher values of slump, air content, and bleeding rate were linked to greater rebound amounts. Conversely, rheological properties of shotcrete mix, specifically plastic viscosity, and yield stress, exhibited an inverse relationship with rebound generation. This suggests that higher plastic viscosity and yield stress values were linked to reduced rebound quantities [17]. Results obtained from conducting experiments determining the relationship between rebound rate and rheological properties are summarized in fig. (11).
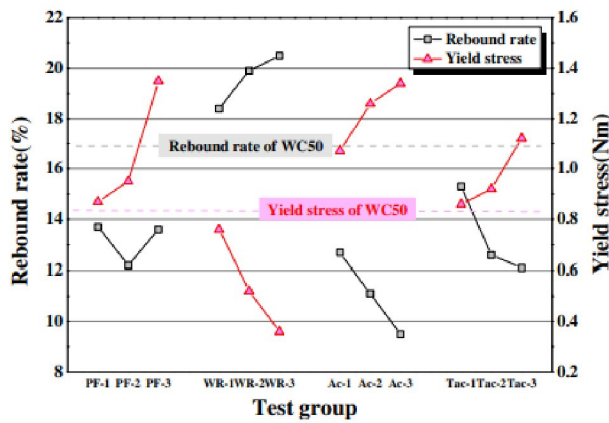
(a)
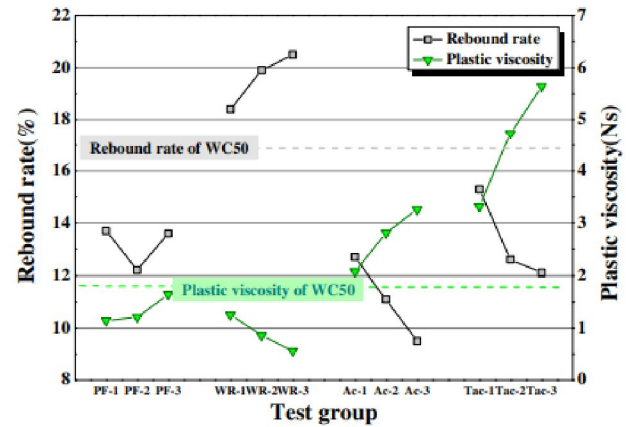
(b)
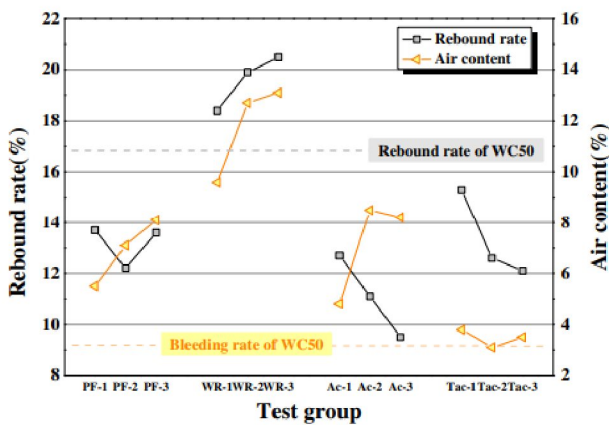
(c)
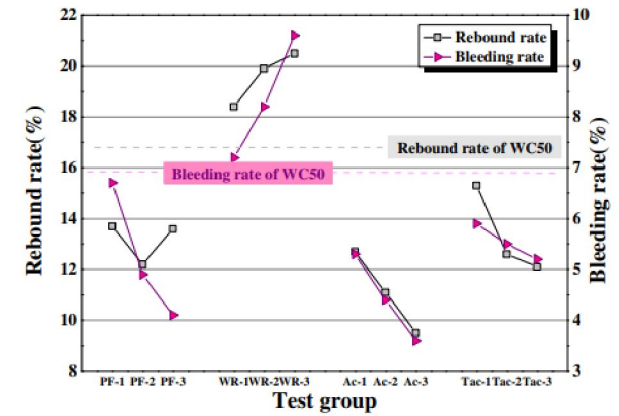
(d)
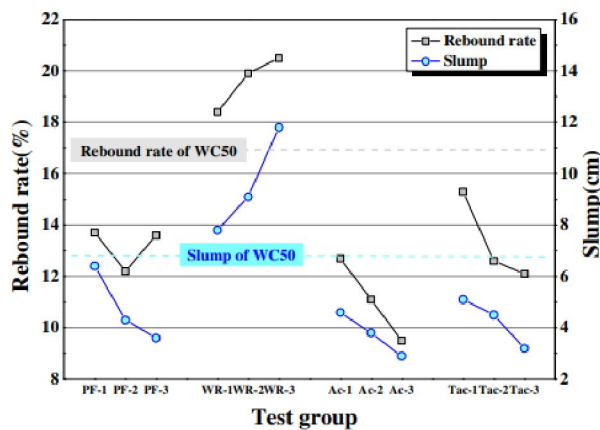
(e)
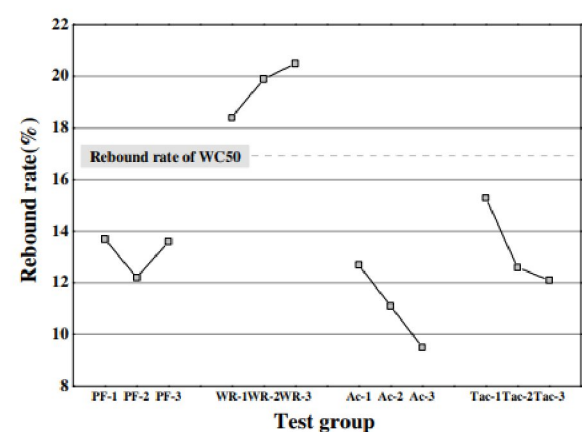
(f)

Figure 11. Results correlating rebound and shotcrete yield stress as follows: (a) plastic viscosity, (b) air content (c) bleeding rate, (d) slump, (e) application of different admixtures, and (f) modified results [15].

Results from fig. (11) indicate that specific characteristics of freshly mixed shotcrete can act as indirect indicators of rebound in the shotcrete. For example, shotcrete blends featuring increased slump, air content, and bleeding rate might exhibit greater rebound tendencies, while mixes with elevated plastic viscosity and yield stress could display diminished rebound. Comprehending the connections between these mix properties and rebound aids in fine-tuning shotcrete mix formulations and spraying conditions to mitigate rebound, thereby enhancing shotcrete effectiveness during application [15].

Rebound can also be affected by the operator skill or the efficiency of spraying nozzle and equipment, therefore physical parameters like air pressure and base mix flow are also important [16]. The use of bio-based admixtures, such as Microfibrillated Cellulose studied in this thesis, may have the potential to improve shotcrete properties and reduce rebound, resulting in cost-effective and efficient shotcrete placement processes.

2.4.2 Cured state performance measurement

In its cured or hardened state, shotcrete mortar performance is measured from its mechanical properties based on Compressive and Flexural strength. The progression of strength in shotcrete can be categorized into three distinct stages of specimen preparation: very-early strength (0-2 hours), early strength (24 hours), and final strength (7 to 28 days), as illustrated in fig. (12) [6].
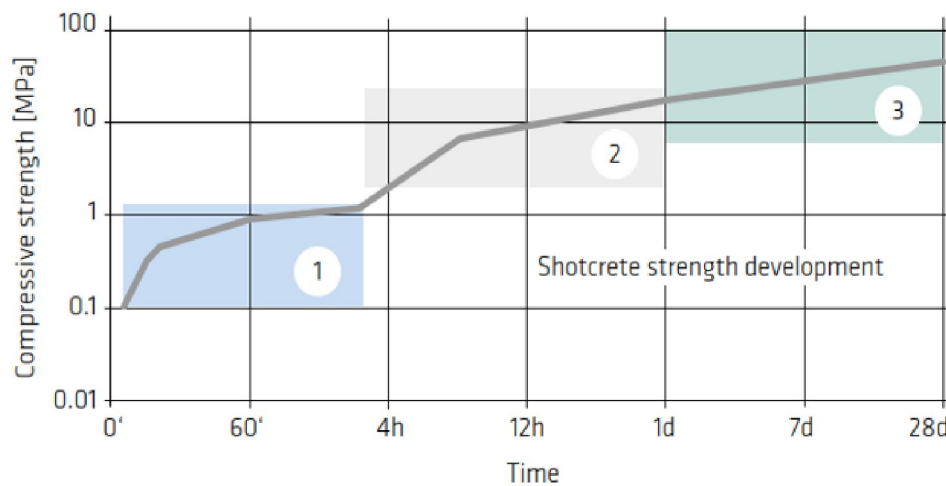
Figure 12. Strength development of shotcrete during three phases: (1) very-early strength, (2) early strength, and (3) final strength [6]

Compressive strength is defined as the maximum axial load that a material can withstand before it is subjected to failure. In shotcrete, this property reflects its ability to absorb applied loads while maintaining its structural integrity [6]. Measuring the compressive strength of shotcrete mortar provides valuable information about its overall strength and durability, which are critical factors for its performance in various applications, such as rock reinforcement, tunneling, slope stabilization, and structural repairs [18].

Flexural strength is a measure of the load that shotcrete can bear against bending or flexural loads and maintain its structural integrity over such conditions. This showcases the ability to resist bending loads and tensile stresses. Flexural strength is an important mechanical property of shotcrete, as it provides information about its ability to withstand applied loads without cracking or failing in bending or tensile modes, especially during its application in beams [18].

Assessing the compressive and flexural strength of shotcrete involves subjecting the prepared mortar samples for each test in the Universal Testing Machine (UTM) and applying compressive and flexural load until failure [6]. Both compressive and flexural loads are also represented as yielding stress on their respective stress-strain curves as shown in fig. (13).
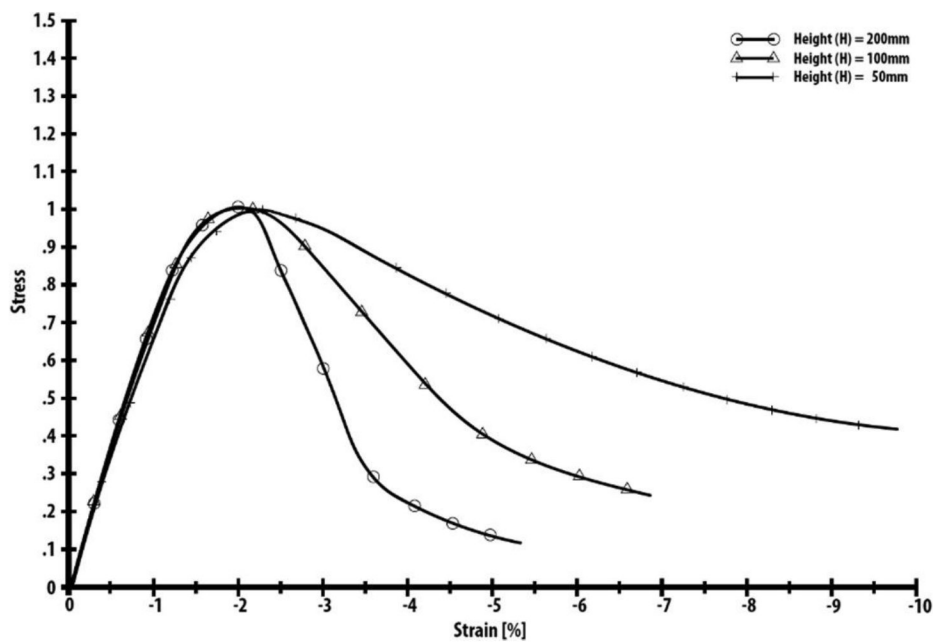
Figure 13. Typical stress-strain curve for compressive and flexural strength test [19].

3 Objectives and scope of this study

The primary objectives of this dissertation are as outlined as follows:

i. Review the shotcrete performance measures based on established research.

ii. Assess the compatibility and performance of MFC admixture in different shotcrete mix designs, with focus on physical, mechanical, rheological, and chemical properties.

The scope of this research encompasses the preparation of different shotcrete samples representing distinct mix compositions based on the dosage of MFC, followed by rigorous laboratory testing and subsequent analysis of the obtained results.

4   Research Methodology

4.1   Description of materials

4.1.1   Ordinary Portland Cement (OPC) Type 1

The term 'cement' can be elucidated as a material substance characterized by its inherent capacity to chemically bind together various materials through a range of different reactions, aided mainly by water in controlled amounts [20]. Portland cement is the most common type of cement with an annual worldwide production reaching approximately 3.8 million cubic meters. Cement is composed of a variety of chemical compounds as shown in table (3).

Table 3. Chemical composition of ordinary Portland cement [21].

Component	Amount
Lime (CaO)	60.00-67.00%
Silica (SiO_2)	17.00-25.00%
Alumina (Al_2O_3)	3.00-8.00%
Iron oxide (Fe_2O_3)	0.50- 6.00%
Magnesia (MgO)	0.50- 6.00%
Sulphur trioxide (SO_3)	1.00-3.00%
Soda and/or Potash (Na_2O+K_2O)	1.00-3.00%

For this research RAPID$^®$ Aalborg Cement – CEM 1 (strength class 52.5 MPa) has been utilized as the primary binder for all experimental tests. It finds its versatile applicability in a wide array of concrete applications in all environmental classifications. Primarily employed in ready-mix concrete, its accelerated strength development renders it suitable for the production of concrete and related constructs including pavements, reinforced concrete structures, bridges, railway edifices, reservoirs, tanks, culverts, sewers, water pipes, masonry components [22].

4.1.2   Silica fume

Micro silica, commonly known as silica fume or condensed silica fume, is a by-product of silicon or ferrosilicon metal, produced as a gaseous by-product during the reduction process of pure quartz. This vaporized gas undergoes condensation within bag house

collectors, resulting in the formation of very fine powder comprised of spherical particles [23], with additional characteristics shown in table ().

Table 4. Physical characteristics of Silica Fume [23].

Physical characteristics	Value
Diameter	01 – 0.2 microns
Surface area	30000 m²/kg
Density	150 – 700 kg/m³
Appearance	Grey gunpowder

Elkem Microsilica® 920D (variant D-densified) silica fume has been used throughout the experimental set up and tests. Its properties are in accordance with the EN 13263 standard. Upon application into the shotcrete mix, it contributes to the enhancement of the concrete and mortar formulations. It physically acts as a particle packing optimizer in the concrete mortar mixture whilst chemically acting as a highly reactive pozzolan. Some of its benefits include, (1) higher compressive strength, (2) increased durability, and (3) improved rheology [24].

4.1.3   Aggregate

Sand acts as a pivotal component in concrete composition, contributing to its structural integrity and overall performance. Its primary function involves providing bulk and stability to the mixture, thereby facilitating a more rounded and balanced distribution of forces [25]. It also contributes to controlling the overall water-to-cement ratio due to the inherent moisture content, thereby having influence on the mechanical strength and overall durability. Shrinkage and cracking tendences in concrete are also mitigated due to the usage of proportionate quantities of sand, thereby enhancing the service life and long-term resilience of structures [26].

Natural sand has been used as the primary aggregate for all shotcrete mortar design-mix preparation, with a ratio of 1:4:1, in the aggregate sizing of 0-8mm. The moisture content for the sand used was between 0.22% to 0.55% tested during all mortar design-mix preparation. Sand particle size, moisture content, and cement to sand ratio is crucial for preparing a shotcrete mix design that allows for optimum pumpability.

The moisture content in sand was calculated in accordance with ASTM D2216-19 standard [27]. Following procedure was adopted: (1) The sample sand was initially weighed (W_i) at 0.5 kg, (2) The sample was then heated gently for 5 minutes ensuring that the heat is evenly distributed, (3) The heated sample is then weighed (W_d) and the difference in

weight is recorded, (4) Process is repeated until the difference in weight is negligible, (5) Moisture content is then calculated as a percentage of initial and final weight.

Sample calculation of the used sand is as follows:

Initial weight (W_i) = 500 g

1st weight after heating (W_{d1}) = 498.9 g

2nd weight after heating (W_{d2}) = 498.9 g

3rd weight after heating (W_{d3}) = 498.5 g

Since there is no change in weight after heating therefore W_{d3} is the final weight of sand (W_d).

Therefore,

$$Moisture\ content\ (\%) = \frac{W_i - W_d}{W_i}\ x\ 100$$

$$Moisture\ content\ (\%) = \frac{500 - 498.5}{500}\ x\ 100$$

$$Moisture\ content\ (\%) = 0.3\%$$

4.1.4   Superplasticizer

Superplasticizers, also referred to as high-range water reducers, are chemical based admixtures used in the mix-design recipe for the enhancement in workability, and improvement in flow without making any significant impact to the water-to-cement ratio (w/c), or the overall strength of concrete or shotcrete. Due to the nature of their impact, they are quite useful in designing shotcrete mixes, which cater to high-strength, durable and flowability [28]. Their functionality is based on dispersion of cement particles and solid materials in the mix, reducing the internal friction between these particles. The outcome therefore, is improvement in flowability, high dosing efficiency, short mixing time, cohesiveness, and increased slump, rendering the shotcrete to be easily pumped, placed, and compacted [29].

For this research, Sika® ViscoCrete®-4028 SC has been used as a superplasticizer for all shotcrete mortar mix-designs, with specification mentioned in table ().

Table 5. Data sheet specification of Sika® ViscoCrete®-4028 SC [16]

Specification	Value
Density	1.06 ± 0.02 kg/l (at +20°C)

pH value	5.5 ± 1.0
Conventional solids content	$28.0 \pm 1.0\%$
Total chloride content	$\leq 0.01\%$ (chloride-free)
Sodium dioxide equivalent	$\leq 0.8\%$ Na 2 O equivalents
Optimum dosage	0.2%-0.5% (based on binder content)
Appearance	Greyish white liquid

4.1.5 Microfibrillated Cellulose (MFC)

Cellulose is a naturally occurring biopolymer that provides trees and plants with their inherent structural integrity [30]. Its importance lies in its abundance as a biopolymer in nature, with wood fibers being the most utilized form of cellulose in industry. As depicted in figure (), the elemental fibril elementary fibril's length measures several micrometers, while its diameter spans from 4 to 200 nanometers [31].
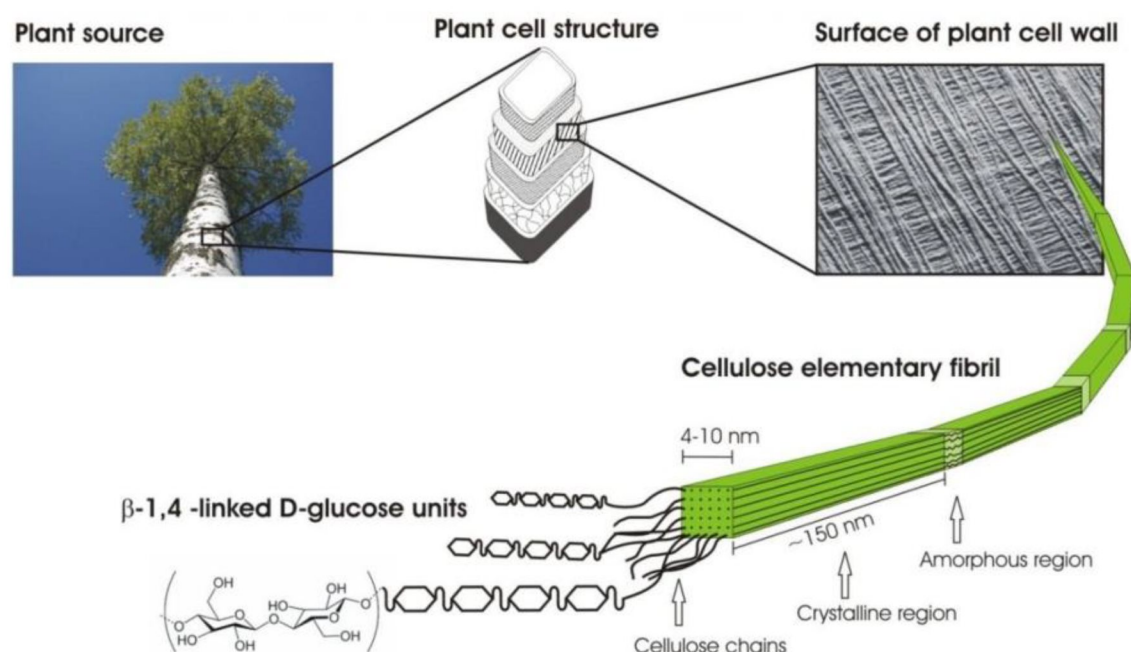
Figure 14. Microfibrillated cellulose (MFC) source and nano-sized fibers structure [31].

By employing a specialized technique, nanoscale cellulose fibrils and bundles are isolated and generally refined from wood pulp during the refining process [30]. Once fully separated, these fibrils create densely viscous dispersions in water, owing to their remarkably extensive surface area and hydrogen bonding. Approximately 20% of the fibril's atoms are positioned on its surface, allowing them to engage in hydrogen bond interactions with

adjacent water molecules [31]. Microfibrillated Cellulose (MFC) in terms of gel and its Scanning Electron Microscopic (SEM) image is presented in fig. (15).
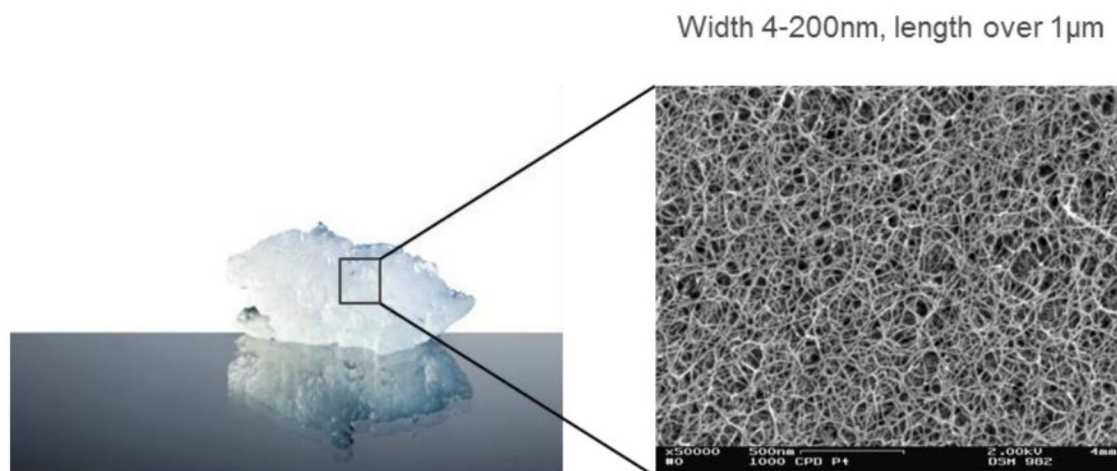
Figure 15. MFC gel structure and its SEM imaging [31].

Due to their promising potential as an efficient rheology modifying agent in concrete and cement grout applications, they are a great source of research in shotcrete applications in terms of addressing the rheology and rebound problems [30]. In this dissertation, the effect of MFC hydrogel is investigated in shotcrete mix-designs, which are produced from Norwegian Spruce.

4.1.6   Water

Water is not only used to aid in the design mix, but it has a significant impact on the properties, behaviour, and performance of the final shotcrete material. The role of water is encompassed over several key aspects: (1) it allows for improved workability, rendering to smooth delivery and adherence to surfaces, (2) in optimum quantity it helps obtain consistency with the desired viscosity, and (3) addition of water initiates the Hydration reaction between cement and water thereby generating binding effect, and proper adhesion [32].

When preparing a mix-design, special care is given to the water-to-cement ratio, which has a significant influence on the performance, strength, and overall quality of the resulting shotcrete design. It is the ratio of the water quantity used relative to the mass of cementitious or binder material (in this case cement and silica fume) [33].

4.2 Mixing methods

4.2.1 Shotcrete mortar

Table (6) shows the mix design based for all shotcrete mortar samples with different concentrations of MFCP01-L MFC as an additive.

Table 6. Breakdown of the shotcrete design-mix.

Material	Name	Reference	MFC 0.1%	MFC 0.25%	MFC 0.5%	MFC 0.75%	MFC 1%
Cement	Aalborg Rapid Cement (CEM I)	5579	5579	5579	5579	5579	5579
Silica Fume	Elkem microsilica 920D	294	294	294	294	294	294
Aggregate*	0-8 mm	22618	22618	22618	22618	22618	22618
Superplasticizer	Sika Viscocrete 4028-SC	83	83	83	83	83	83
Exilva	P 01-V (10% fibrils)	-	6	15	29	44	59
Water	-	2819	2813	2804	2790	2775	2760
Total (g)		**31383**	**31383**	**31383**	**31383**	**31383**	**31383**

This dosage is based on the density of 1 cubic meter of shotcrete, as shown below.

$$\frac{313.83\ kg}{15\ L} = 21\ kg/m3$$

As shown in table (6), these mix designs are based on satisfying the water-to-binder ratio (w/b), superplasticizer concentration, silica fume dosage, MFC ratio, as well water being adjusted for as per the concentration of MFC in the mix to maintain w/b.

Table 7. List of defining parameters in the design -mix need to be satisfied.

Parameter	Ratio in the shotcrete mix
Water to binder ratio w/b (b = cem + SF)	0.48
Super Plasticizer dosage	1.2% (sbwb)
Silica Fume dosage (sbwc)	5.3 %
MFC dosages "as delivered"	sbwb
Water	adjusted for MFC only not moisture from aggregate

Where, sbwc is the solids by weight of cement, referred to as the ratio of the mass of non-cementitious materials to the mass of cement in a mixture, expressed as a percentage. And sbwb is the proportion of the mass of non-binder components to the mass of the binder in a mixture, presented as a percentage.

Mixing of all the constituent materials was carried out with the concrete mixer at the Østfold University College. Following protocol was employed for all the mix-designs: (1) Moist the mixing barrel from inside, (2) Add aggregate and cement and mix them for 60 seconds, (3) Add water and Super Plasticizer (SP) mixture and run the barrel for 90 seconds, (4) Add Silica Fume (SF) into the mix and run for 90 seconds, (5) Stop and check for proper mixing of the material (i.e., no dry material should be on the walls of the barrel), (6) Add MFC all together in the mix and run for 120 seconds. The total time for the sample preparation was set to be 360 seconds. Figure (16) shows the cement mixer used for mortar preparation.

Figure 16. Cement mixer utilized at the Østfold University College laboratory.

4.2.2   Cementitious paste

For all the shotcrete paste specimens, a mix-design consisting of cementitious material (cement and silica fume), water and MFC was employed. Mixing of all these constituents were performed in the laboratory benchtop mixer as shown in fig. (17). The w/b ratio, silica fume dosage, and MFC concentration was kept under satisfactory limit based on the design. Following protocol was used for all paste preparation: (1) Moist the benchtop mixer pot from inside, (2) Add cement, silica fume, and Exilva. (3) Add water in the mix (note the time, in case of rheology tests to maintain paste freshness for the test within 15 minutes), (4) Run the mixer at 140 rpm for 120 seconds, (5) Stop and check for proper mixing, and (6) Run the mixer at 245 rpm for 120 seconds. The total time for this mixing was set to be 240 seconds.

Figure 17. Cement benchtop mixer at Østfold University used to prepare shotcrete paste.

4.2.3   Casting and curing of samples

Post mixing, the shotcrete is casted into different molds to develop mortars for compressive and flexural test specimens. Fig. (18) shows the casted molds from the freshly prepared mixture.

(a)   (b)
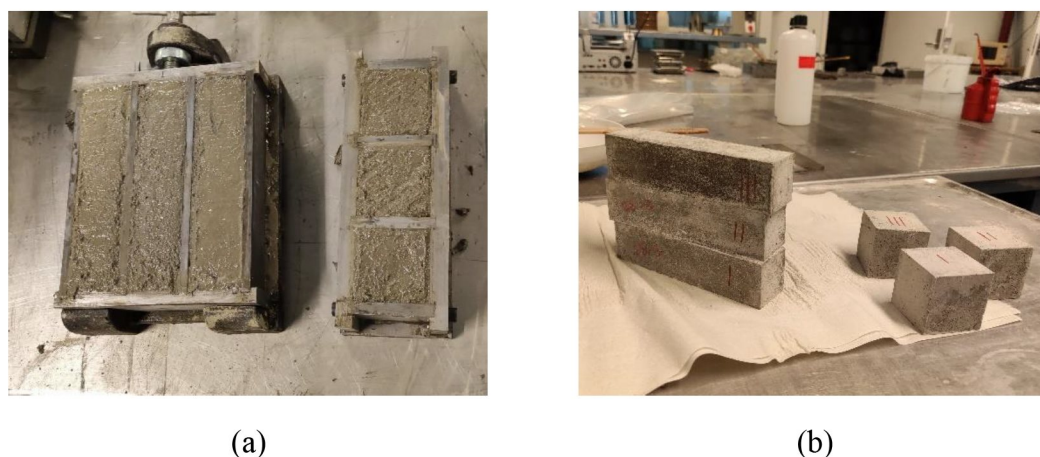
Figure 18. Shotcrete mortar sample preparation at Østfold University College laboratory; (a) being cast (b) cured mortar blocks ready for testing.

In this research, three molds of $50 \times 50 \times 50$ mm3 were used to cast mortars for compressive strength tests, while three molds of $40 \times 40 \times 160$ mm3 were utilized to cast mortars for flexural strength evaluation. In each case, the samples were carefully processed through a vibration machine to remove any entrapped air in shotcrete inside the molds.

Curing is a process used for catalysing the hydration process of cement and is related to the temperature control and movement of moisture from and into the concrete or shotcrete mortar [34]. As shown in fig. (19), exposing the mortar by curing it in the body of water keeps the mortar saturated and allows for continuous hydration of cement and strength gain. Due to this relation the strength gain stops once the curing is completed [34].
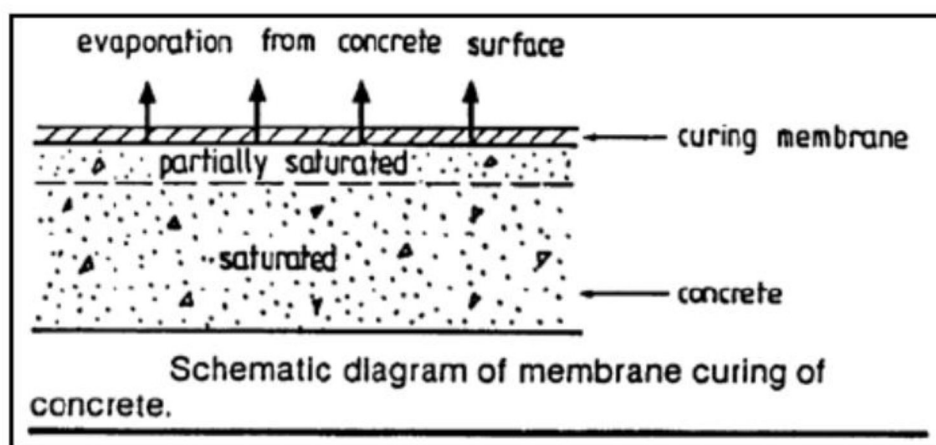
Figure 19. A schematic of the curing process via immersion method [35]

It is important to ensure adequate moisture in cement since cement hydration halts at relative humidity of <80% inside the capillaries [34]. Environment exposure of concrete results in evaporation resulting in loss of internal moisture thus reducing the initial water-to-cement ratio, giving rise to incomplete hydration, hence lowering the quality of

concrete in terms of undesirable strength, and impermeability in the product concrete, giving rise to a phenomenon called early drying of concrete, which cause micro or shrinkage cracks on the surface [36]. In this thesis, the immersion or pond curing method was utilized at 20 °C.

4.3   Testing methods

4.3.1   Flow table tests

Flow table test is a standard procedure utilized for evaluating the workability and consistency of freshly prepared concrete or shotcrete. Through this test, the flow and spread of shotcrete can be determined, which is vital for understanding the rebound effect due to spray application. These tests include calculating the slump height and flow [37]. Figure (20) illustrates the flow table set up as per ASTM C143/C143M-20 industrial standard.
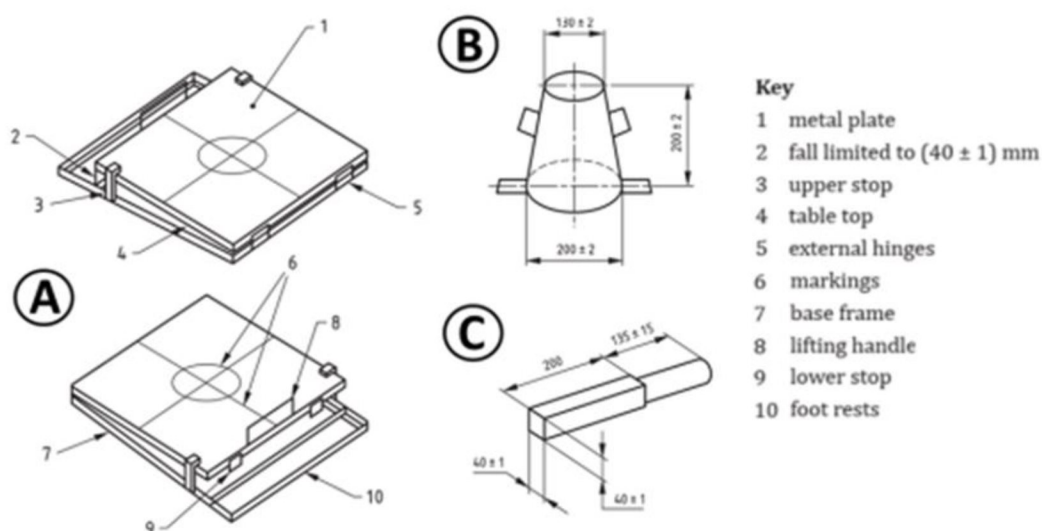
Figure 20. Flow table equipment as per ASTM C143/C143M-20 and EN 12350-5 [38].

This test consists of the following two phases: (1) slump height measurement, and (2) slump flow measurement. The test method is based on placing the flow table on a flat ground with its surface moistened, and the test cone placed at the center of the table. The freshly prepared shotcrete mix sample is then filled inside the cone and compacted with the tamping bar. The cone is filled in three steps, with each step involving compacting procedure with the tamping bar when the cone is filled up to 25%, 50% and 75% respectively. After filling, the cone is then removed, and the slump height is measured relative to the cone length and the recorded difference is called the slump [38].

$$Slump\ height\ (h) = Cone\ length - Mortar\ height$$

After the slump height is calculated, the slump flow can be performed as per NS-EN 12350-5:2019 standard. In this test, the table is raised from its hinges and dropped to a

total of standard 15 times to allow the shotcrete slump sample to flow. The diameter of the flow is recorded in perpendicular directions and the mean reading is the flow of the shotcrete sample as shown [39].

$$f = \frac{d1 + d2}{2}$$

Where f is the mean value of flow (mm), d1 is the maximum dimension of flow in 1st direction (mm), and d2 is the maximum dimension of flow in 2nd direction (mm) perpendicular to d1 [39].

For the mortar flow table test, a mini automated flow table device was used. This test was performed under the ASTM C1437-20 standard. This test involves filling the freshly prepared shotcrete sample in the mini cone, on the flow table, and using tamping the shotcrete under standard procedure. The cone is then removed, and machine is run then run under timer of 15 seconds. The diameter of the flow is recorded in perpendicular directions and the mini slump is recorded as the mean reading [40].

4.3.2   Air-content test

The air content of shotcrete is assessed using a pressure gauge meter in accordance with the NS-EN 1015-7:1998 standard, as illustrated in Figure (22). The pressure gauge meter consists of four components: (1) an 8-liter air test container, (2) a cover assembly, (3) a pressure gauge, and (4) an air pump.[41].
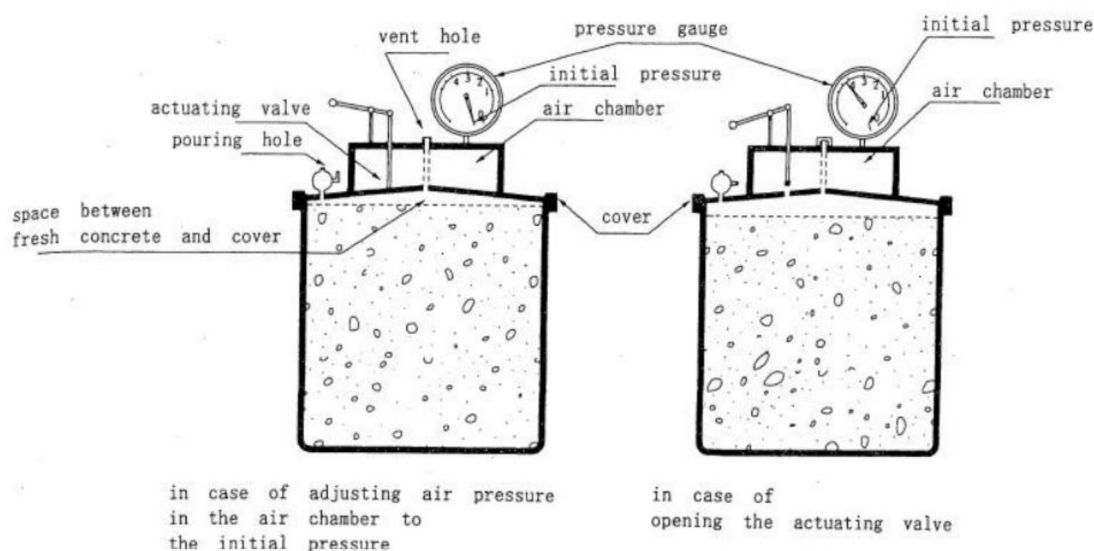
Figure 21. Apparatus for air content test [41]

Following procedure was utilized to determine the air content in shotcrete samples: (1) filling of test container with freshly prepared shotcrete sample with tamping rods to release entrapped air, (2) gentle tapping of the container with mallet, (3) fixing the cover over the container and sealing with cover clamps, (4) addition of water from the air valve

to provide sealing and then closing these valves, (5) pumping the air into the container using the air pump valve until the gauge's designated pressure limit is reached, (6) releasing the air through the main air valve, and (7) recording the air content % after the pressure subsides.

4.3.3   Compressive strength

The measurement of compressive strength is generally carried out via destructive testing, where shotcrete mortar specimens, in the form of cubes, are placed under axial loading till failure. The material's compressive strength is calculated with the help of a Universal Testing Machine (UTM) using the resultant load at failure as shown in fig. (23) [42, 43].
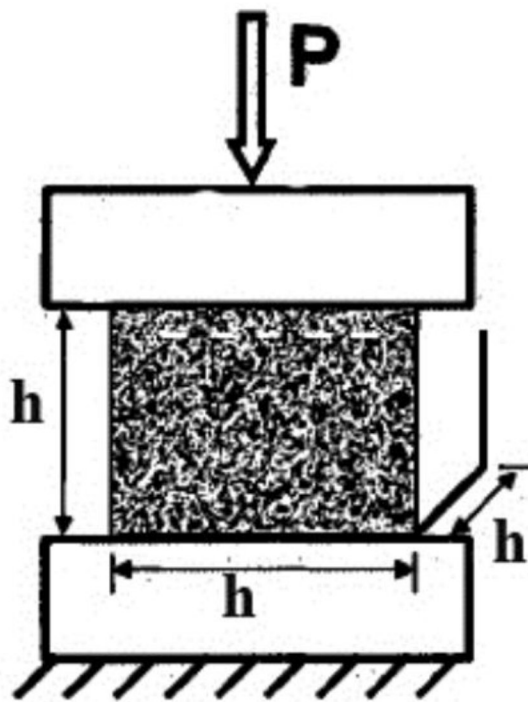
Figure 22. Compressive strength test schematic [42]

The resultant load at failure is used to calculate the compressive strength as follows:

$$F_c = \frac{P}{A}$$

Where, F_c is the Compressive Strength (MPa), P is the maximum/resultant load at failure (N), and A is the cross-sectional area of the mortar specimen (mm^2) [44].

4.3.4   Flexural strength

Flexural strength is calculated via preparing prismatic or cuboid shotcrete mortar specimens, and tested at the Universal Testing Machine (UTM) under three -point loading test method outlined in ASTM C348-21 standard [45]. The specimen is placed horizontally on two support points and subjected to a concentrated load at the center. This load induces

bending load on the specimen till rupture [44, 45]. Fig. (24) illustrates the test setup on the UTM bench.
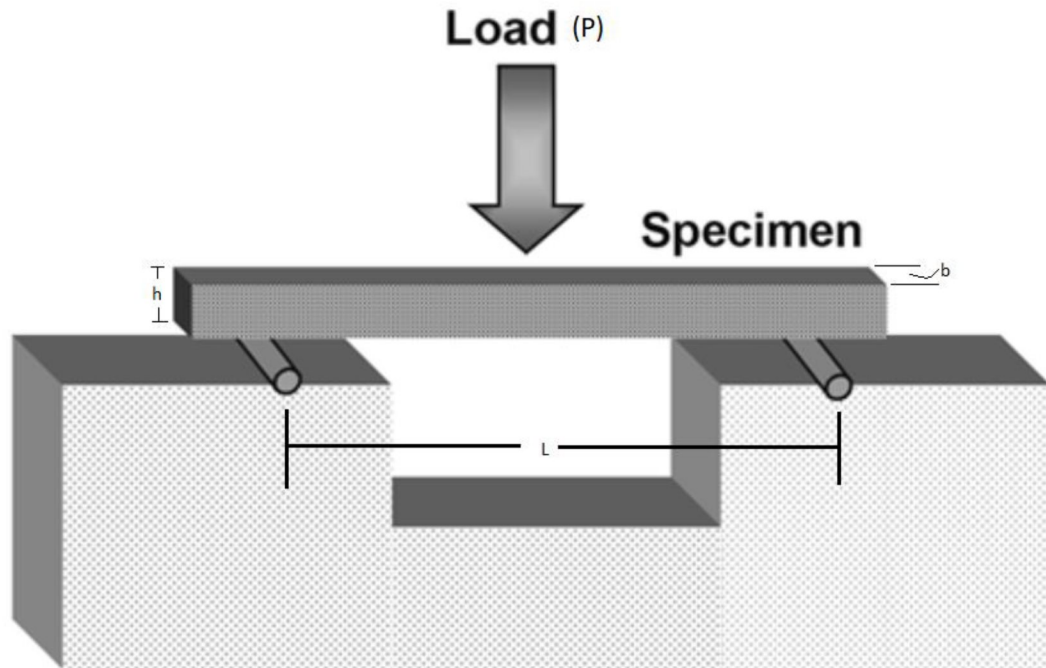
Figure 23. Flexural strength test schematic [44]

The load at failure, along with the dimensions of the specimen, is used to calculate the flexural strength of the shotcrete, as follows:

$$F_f = \frac{3PL}{2bh^2}$$

Where, F_f is the Flexural strength (MPa), P is the applied load (N), L is the length between the two support points (mm), b is the width (mm), and h is the specimen thickness (mm) [44].

4.3.5   Setting-time test

The setting time test is based on the determination of time it takes for a freshly applied shotcrete to transition from fluid to a workable hardened state. This is a critical parameter since it affects the workability, placement, and curing of shotcrete [46]. This test was performed using the automatic Vicat-needle apparatus (Vicatronic E044N) as per NS-EN 196-3:2016 industry standard, as shown in fig. (25).

(a)   (b)
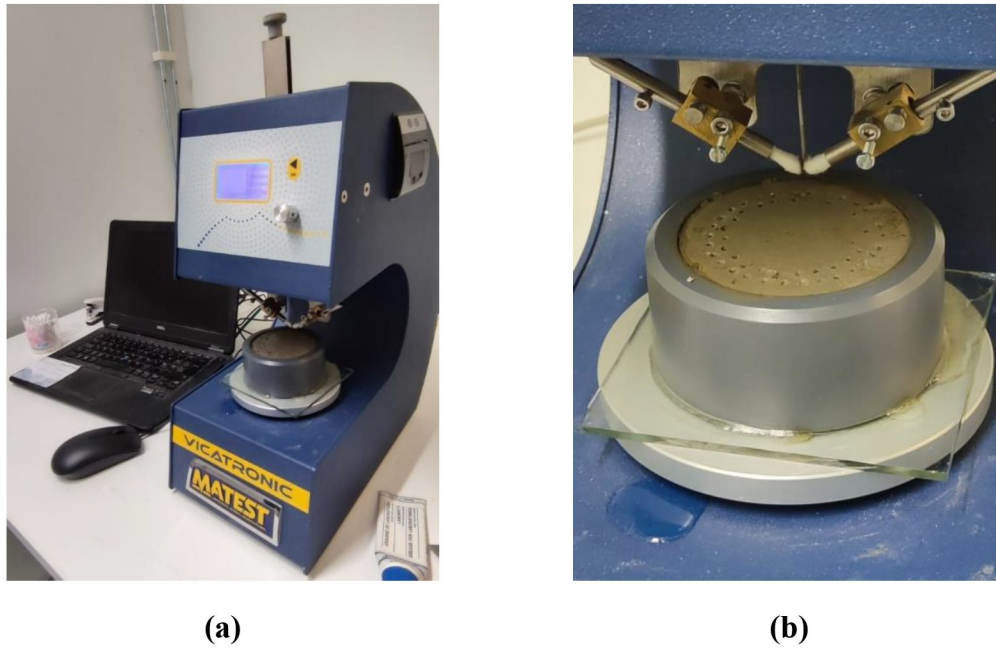
Figure 24. (a) Automated Vicat-needle apparatus; (b) shotcrete paste test mold prepared during the setting time test at Østfold University College laboratory.

Results from this test are recorded in terms of the establishment of initial setting and final setting times. As per the standard ruling, failure to penetrate 5-7 mm into the cement paste rules the initial setting time, while the final setting time is recorded when the cement paste is completely hardened and the vicat needle fails to leave indentation on the surface [46].

4.3.6   Rheological properties test

Rheology analyses of shotcrete cementitious pastes are conducted to understand the material's flow and deformation behavior under different conditions and get an insight into its characteristics such as Static Yield stress, Dynamic Yield stress, and Plastic Viscosity. These parameters are essential for understanding how the shotcrete will behave during placement, pumping, and other construction processes [47].

The rheological analyses of all shotcrete paste mix-designs were performed on the Anton Paar MCR50 rheometer, using the Special Building Materials Cell (BMC 90) with the modular stirrer ST59-2V-44.3/120, as shown in fig. (26).

(a)   **(b)**   **(c)**
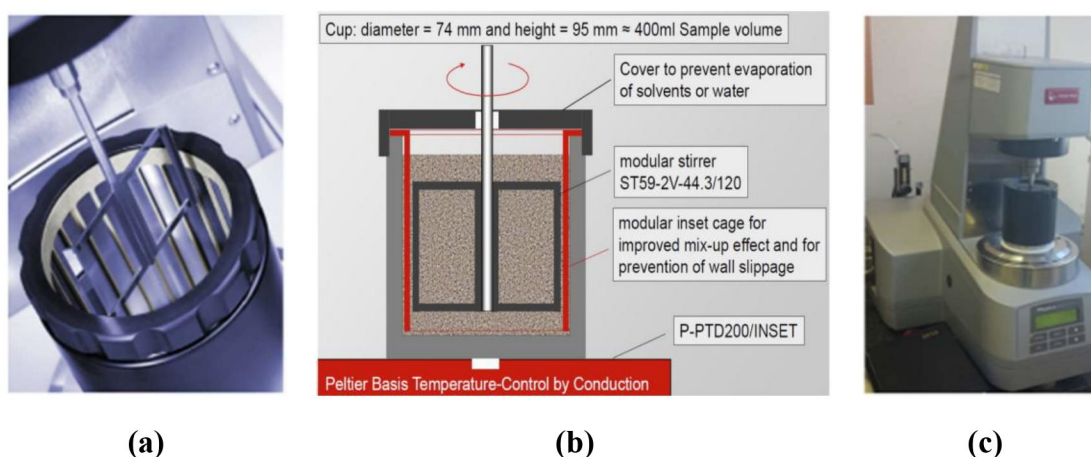
Figure 25. (a) Special Building Materials Cell (BMC 90), (b) Dimensions of BMC 90, (c) Anton Par MCR50 Rheometer [48]

Rheological tests were performed to calculate the static and dynamic yield stress as well as plastic viscosity values, which give an insight to the potential rebound reduction. The shotcrete paste mix-designs were prepared in accordance with the shotcrete cementitious paste preparation mentioned in chapter (3.2.2), and all tests were performed within 15 minutes of sample preparation time to retain similar experimental conditions. Values relating to the static yield stress were calculated measurement recorded from interval 2 of the rheological analyses, while dynamic yield stress and shear viscosity were measured from readings obtained via interval 3 and 4, based on the parameters shown in table (8) [48].

Table 8. Shotcrete paste testing rheological parameters [46].

Interval	Shear type	Measuring range	Time (s)	No. of points	Temperature (°C)
1	Rate	$50 \ s^{-1}$	30 s	30	20
2	Strain	0.001% - 1000%, 1 Hz	60	61	20
3	Rate	$0.01 \ s^{-1}$- $1000 \ s^{-1}$	1000	51	20
4	Strain	$1000 \ s^{-1}$- $0.01 \ s^{-1}$	1000	51	20

4.3.7 Isothermal calorimetric test

Isothermal calorimetric analyses of all shotcrete cementitious paste mix-designs were performed using the Thermometric Analysis Module (TAM) air calorimeter as shown in fig. (27).
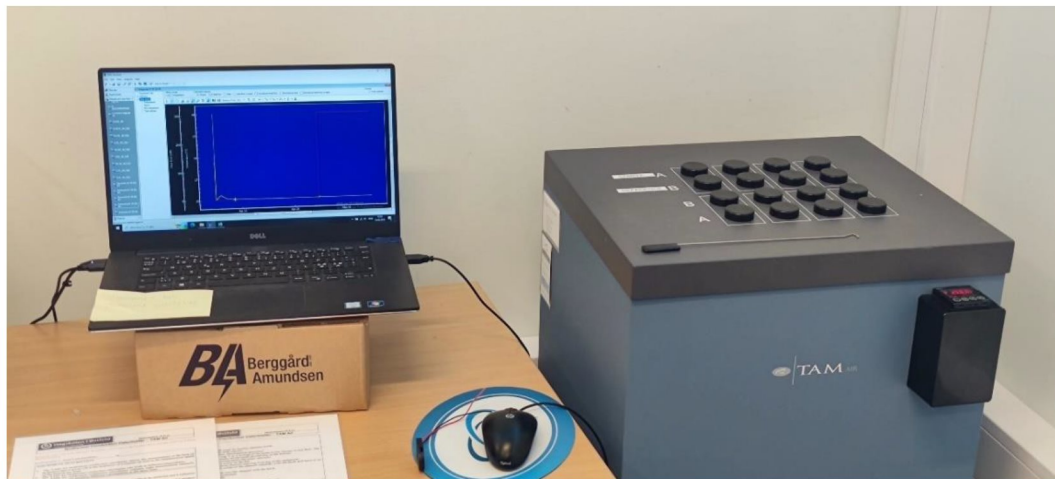
Figure 26. TAM Assistant isothermal calorimeter at Østfold University.

This test is based on measuring the heat generated during the hydration process of cementitious materials. Isothermal calorimetry monitors the exothermic reactions occurring as cement hydrates and sets, and provides insights into the setting and hardening characteristics, hydration rate, and overall cementitious reaction kinetics [49].

Isothermal calorimetric test involves calculating the heat generation rate (P) in a small sample (S) using a heat flow sensor, as heat is conducted towards a heat sink situated within a controlled temperature environment, as shown in fig. (28). This test is performed with a reference sample (R), possessing identical properties (particularly the same heat capacity) to the sample, but not involved in any heat generation. The calorimeter's outcome is measured as the difference between the sample's and the reference signal [50].
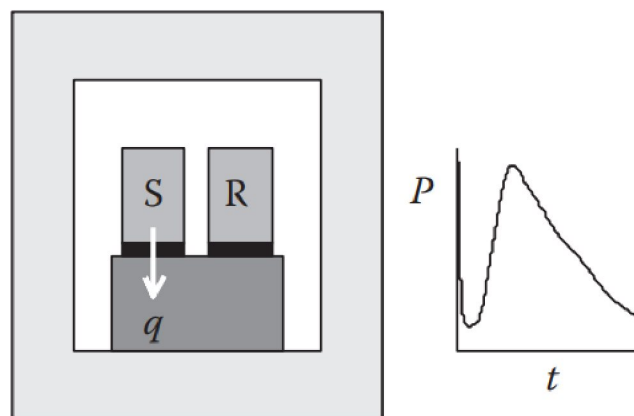
Figure 27. Isothermal calorimetry test schematic [50].

5 Effect of MFC on the physical, and mechanical properties of Shotcrete mix-design

5.1 Flow table tests

Flow table tests were performed to determine the effect of MFC addition on the workability of shotcrete mix designs. These tests, consisting of slump height, slump flow, and mini-slump flow, were performed immediately on the freshly prepared samples at ambient temperature (20 °C).

5.1.1 Slump height

Fig. () illustrates the slump height readings obtained via mixing and analysing the shotcrete mix-designs, in terms of slump height versus control sample and different percentages of MFC addition. The obtained outcomes are comprised of the recorded mean values of the perpendicular slump height (in millimetres) for every preparation of shotcrete in its fresh state, measured immediately after lifting the cone and measuring the deviation of slump relative to the cone height.
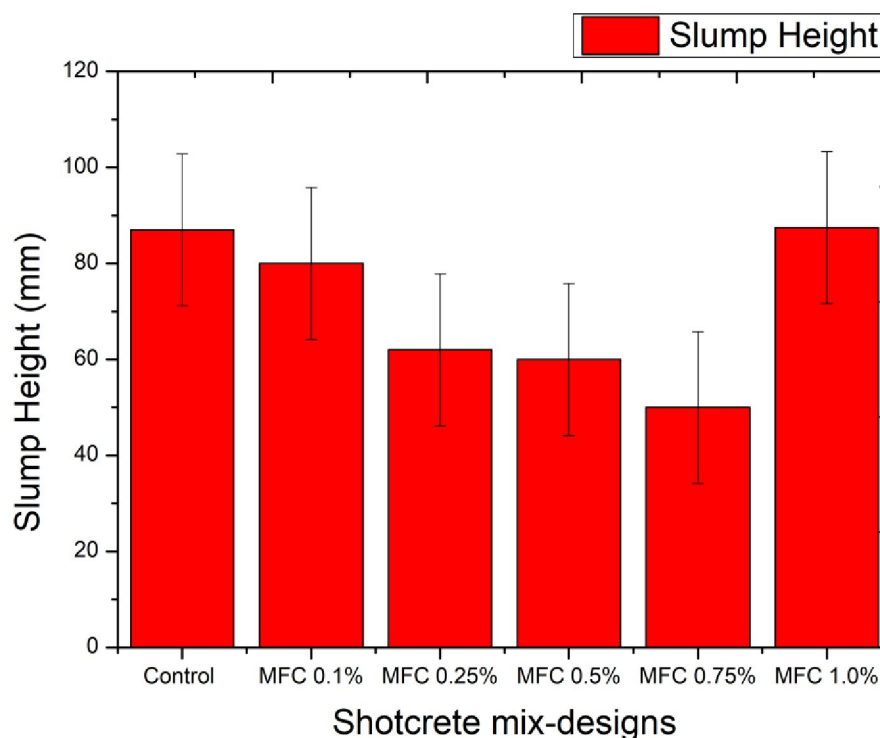
Figure 28. Slump height (mm) for all shotcrete mix-designs tested.

The findings depicted in fig. (28) indicate that the control reference mix has the highest slump height (87mm). Also, it is evident from the fig. (28) that there is a proportional

drop in slump height with a proportional increase in MFC concentration to a maximum of 0.75% of the initial dosage, leading to the lowest value in the slump height. However, beyond 0.75% at the 1% dosage, an anomaly arises, as the slump height appears to rise to a value of 87.5 mm.

5.1.2 Slump flow

The slump flow test was performed immediately after measuring the slump height on the flow table, with manual striking as per the industrial standard ASTM C1437-20, followed by recording the mean values of the slump flow diameters (mm) of each shotcrete mix-design. Fig (29) shows the outcome of each test under different MFC concentration relative to the control shotcrete mix-design.
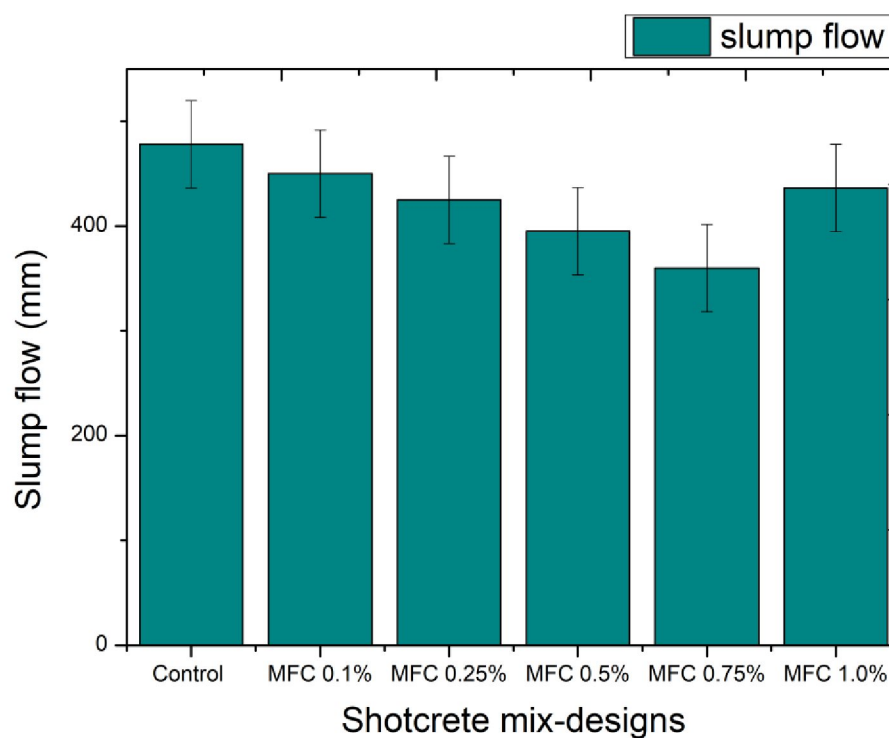
Figure 29. Flow table (mm) results for tested shotcrete mix-designs.

From fig. (), it is evident that shotcrete slump slow tends to decrease with increasing dosage of MFC up to 0.75% per sbwc, compared with the control mix-design. At 1.0% of MFC dosage, an increase in slump flow was observed, keeping in line with its relative slump height.

5.1.3 Mini-slump flow

The shotcrete mortar mix-designs were subsequently evaluated using an automated flow table in accordance with the ASTM C1437-20 standards. Results for the respective shotcrete mix-designs mini-slump flow compared to control mix. are illustrated in Figure (30).
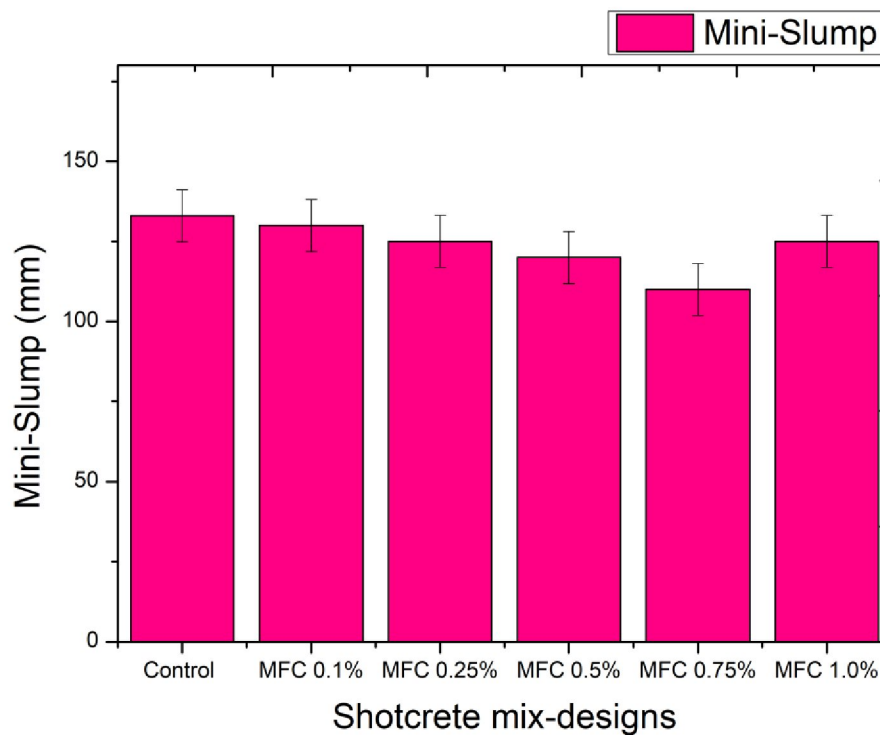
Figure 30. Mini-slump flow (mm) results for all the shotcrete mix-designs tested.

In alignment with the outcomes of the manual slump flow test, similarly it was noted that the slump flow exhibited a decrement with rising concentration of MFC up to 0.75% of the initial dosage. At a 1.0% MFC dosage, a similar incongruity was observed with a sudden increase in slump flow (measuring 125 mm).

5.2   Air content

The different compositions of shotcrete mix-design were assessed using a standard concrete air meter (NS-EN 1015-7:1998). Results were recorded in terms of the air content (%) of each shotcrete mix-design in its fresh state after its sample preparation respectively, as summarized in fig. (31).
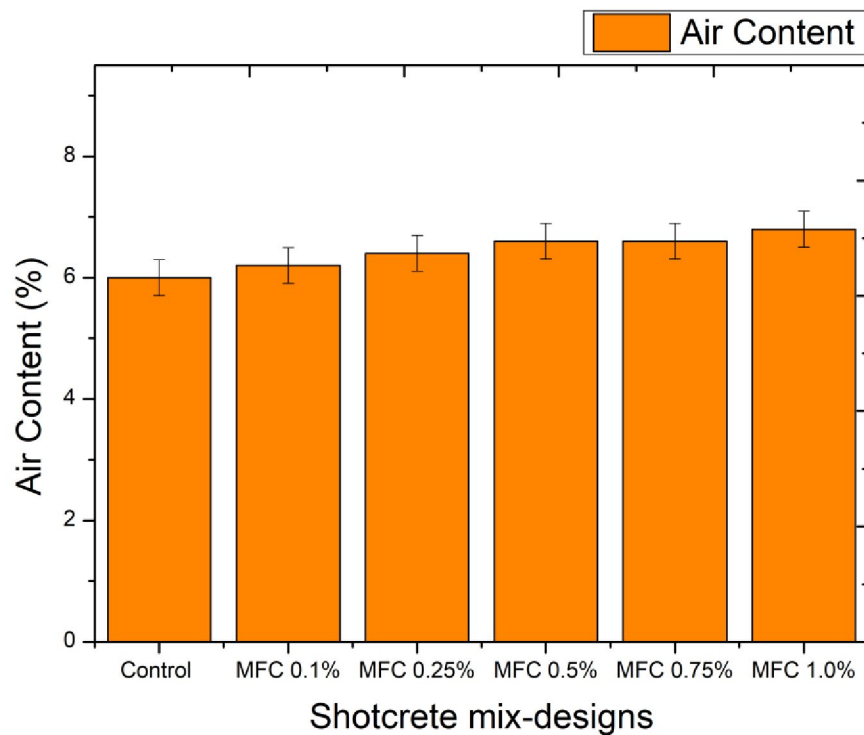
Figure 31. Air content (%) test results of all the shotcrete mix-designs.

It can be seen from fig. (31) that a minor variation in the air-content (%) was observed across the mix-designs, with a slight increase proportional to the increase of MFC dosage.

5.3   Compressive strength

The shotcrete mix-designs were prepared and molded in a cubic specimen (50 mm x 50 mm x 50 mm) with a total of nine samples, three for each of the following testing conditions: fresh mortar state of 24 hours, and underwater curing of 07 and 28 days respectively, with mean values recorded, in accordance with ASTM C109/C109M-20, as shown in fig. (32).
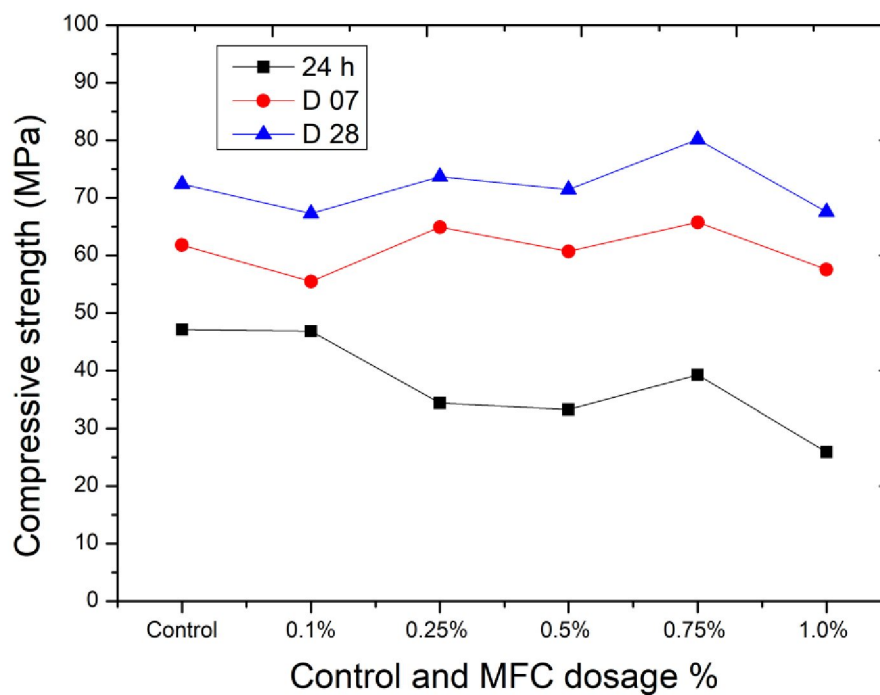
Figure 32. Compressive strength (MPa) results for all shotcrete mix-designs tested.

As seen in fig. (32), the 28 days cured state of final strength tests reveal interesting results. The values obtained at 0.1% - 0.5% dosage of MFC are within the limits of standard deviation of $\pm$ 2-5 MPa. It is to be noticed that the best compressive strength values are obtained at the dosage level of 0.75%, marked by a significant peak (80.13 MPa). The trends at the early strength development at 24 hours and 07 days curing follow similar behaviour.

5.4   Flexural strength

For the flexural strength evaluation, the shotcrete mix-designs were prepared and molded in a cuboid specimen (40 mm x 40 mm x 160 mm) with a total of nine samples, three for each of the following testing conditions: fresh mortar state of 24 hours, and underwater curing of 07 and 28 days respectively, with mean values recorded, as shown in fig. (33).
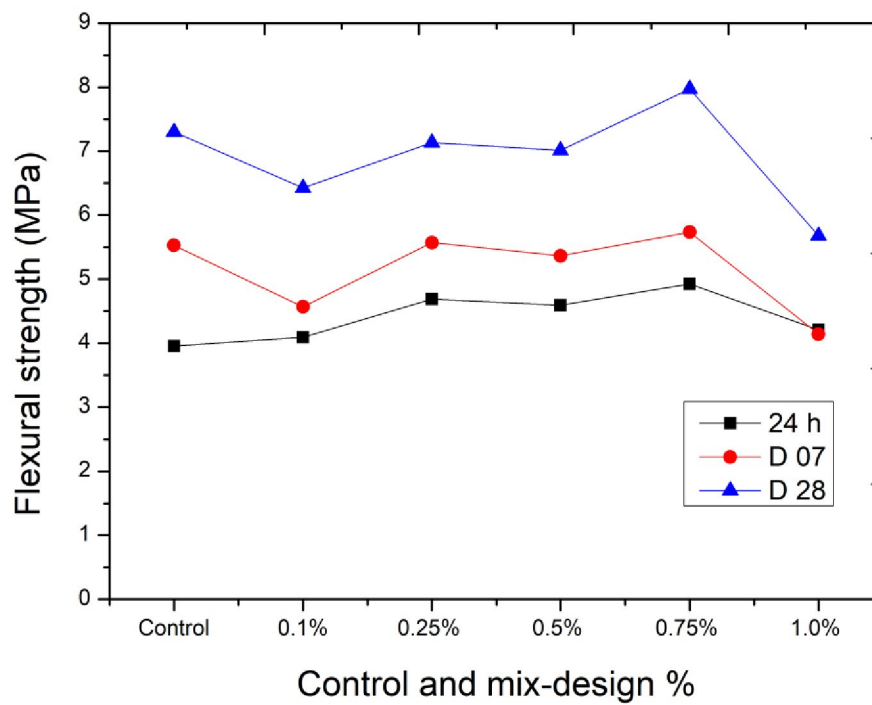
Figure 33. Flexural strength (MPa) results for all shotcrete mix-designs tested.

As seen in fig. (33), at the 28 days cured final strength tests, the values obtained at 0.1% - 0.5% dosage of MFC exhibit minor variation, within the standard deviation of $\pm$ 0.1-0.9 MPa. It is to be noticed that at 0.75% concentration, there is a noticeable increase in flexural strength (7.97 MPa). However, it can also be noticed that beyond this point, there is a plummet in flexural strength recording at 1.0% MFC dosage. The trends at the early strength development at 24 hours and 07 days curing follow similar behaviour.

6   Effect of MFC on the setting time, flow, and chemical properties of Shotcrete mix-design

6.1   Setting time

6.1.1   Initial setting time

As depicted in fig. (34), the addition of MFC into the mix-designs provide a little accelerating effect into initial setting time (on average 25 min of faster initial time compared with control mix), with the lowest times recorded at 0.25% and 0.5% respectively. However, it is to note that these variations are of minor nature and do not significantly alter the setting time.
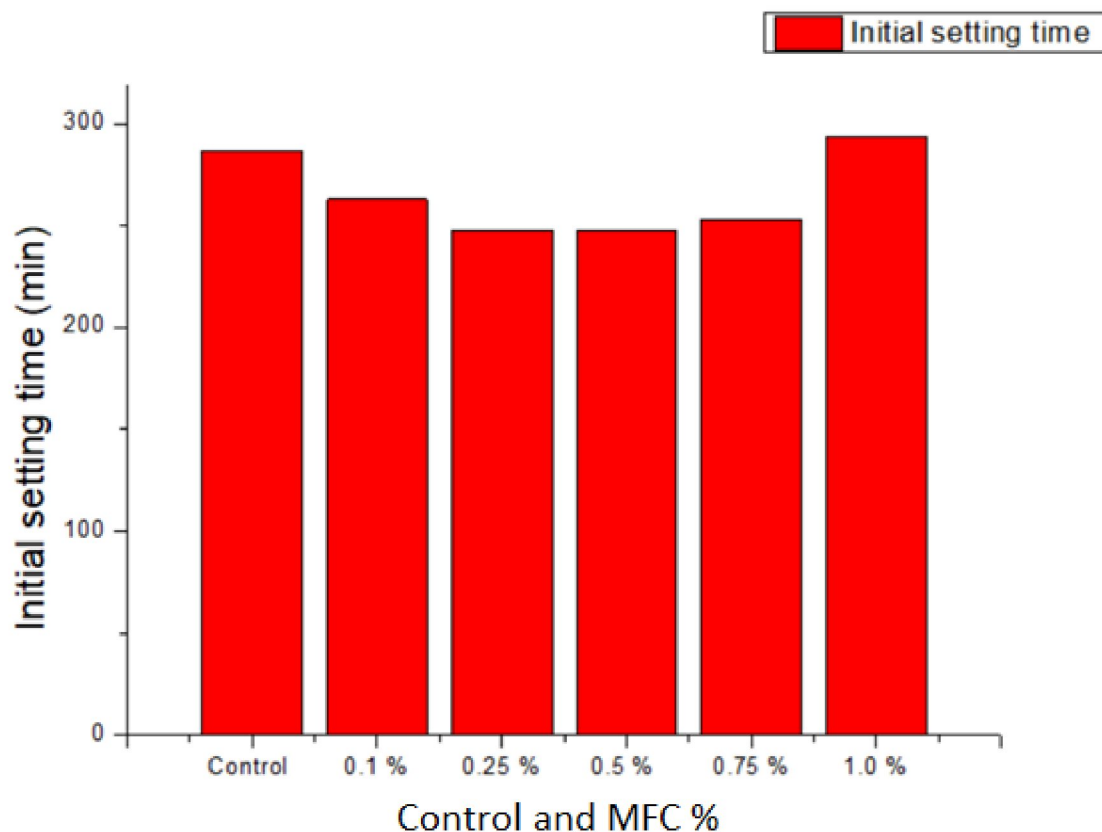
Figure 34. Initial setting time (min) for shotcrete paste mix-designs.

6.1.2   Final setting time

Fig. (35) illustrate the final setting time record for the control and MFC mix-designs. It is evident there is a slight deceleration in final setting time (an average of 17 min delay compared with the control mix) with the increasing dosage of MFC. However, this variation is minor in nature, thus indicating that there is no significant change on the setting time values with the addition of MFC.
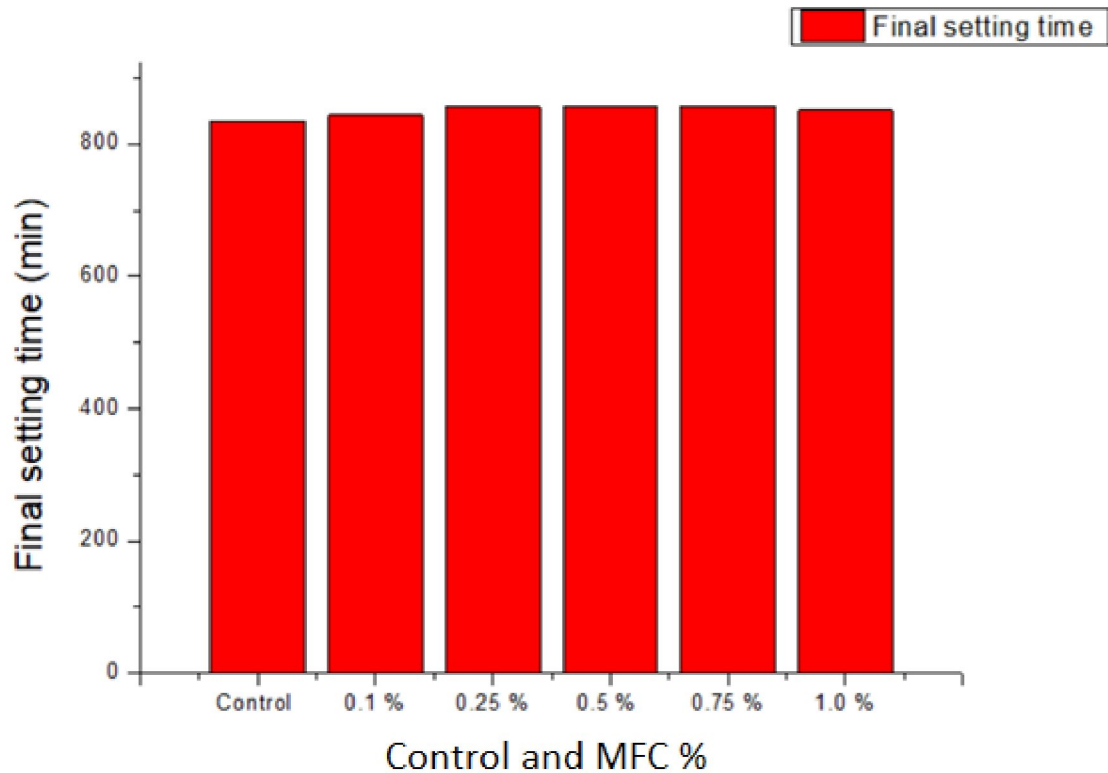
Figure 35. Final setting time (min) for shotcrete paste mix-designs.

6.2   Rheological analyses

6.2.1   Static yield stress

Static yield stress for each shotcrete paste mix design was measured by calculating the yield stress point on the shear stress and shear strain diagram, with results shown in table (9). Shear stress versus shear strain curves for all the shotcrete paste mix-designs are illustrated in fig. (36). All the tests were performed using the measurements recorded during the interval 2 Amplitude Sweep test.
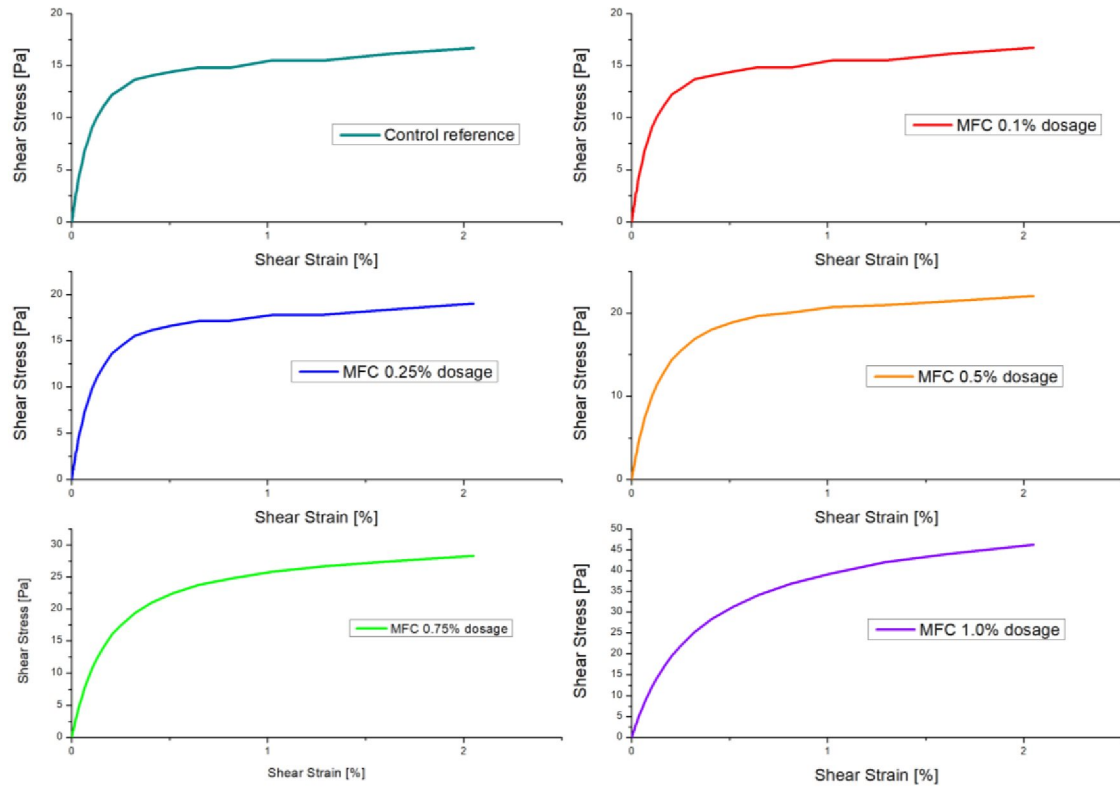
Figure 36. Shear stress vs shear strain diagrams for all shotcrete paste mix-designs.

Table 9. Static yield stress values for all the shotcrete paste mix-designs.

Mix-design	Static yield stress (Pa)
Control reference	4.4
MFC 0.1%	5.7
MFC 0.25%	6.1
MFC 0.5%	6.7
MFC 0.75%	7.3
MFC 1.0%	7.7

From table (9), it is evident that the addition of MFC increases the static yield stress in a linear progression, and that its addition maintains the shear-thinning properties of the shotcrete pastes.

6.2.2   Dynamic yield stress and plastic viscosity

The dynamic yield stress and plastic viscosity were calculated via shear stress vs shear rate curves in the viscosity shear sweep interval 3 and 4 for each sample, as presented in fig. (37), (38), (39), (40), (41), and (42). The nature of these curves indicate that the shotcrete cementitious paste behaves as Bingham fluid [48]. Therefore, using the Bingham model, a linear regression analysis was performed at the yield point of the curve to determine the slope of the curve and y intercept. Then according to the Bingham model, the absolute values are determined with the following equation [10].

$$\tau = \tau o + \mu\gamma$$

Where, τ is the Shear stress (Pa), τo is the Dynamic Yield stress (Pa), μ is the Plastic viscosity (Pa. s), and γ is the Shear rate (1/s) [48].
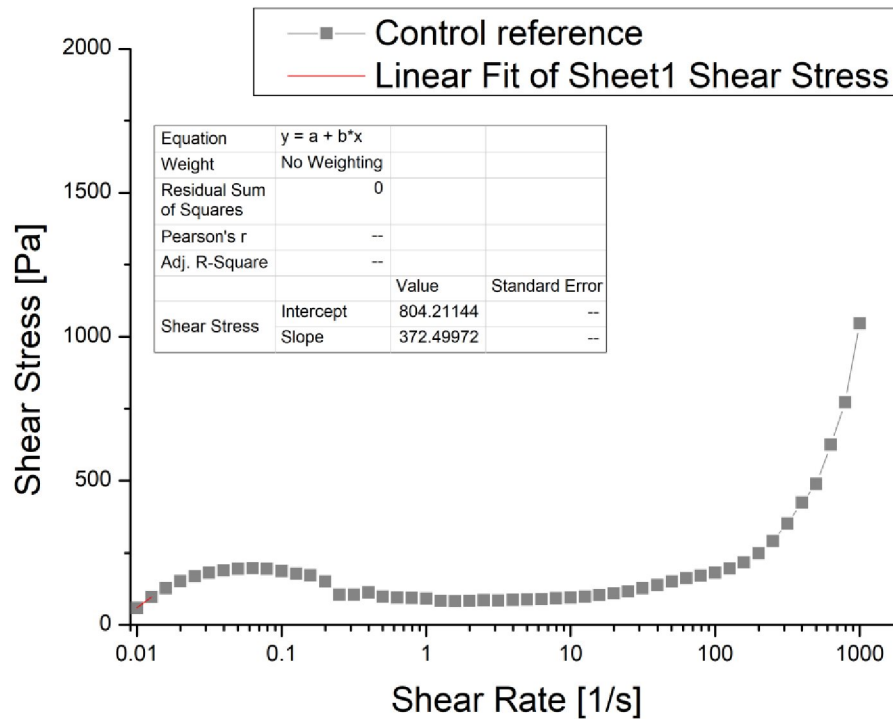
Figure 37. Shear stress vs shear rate curve for control.
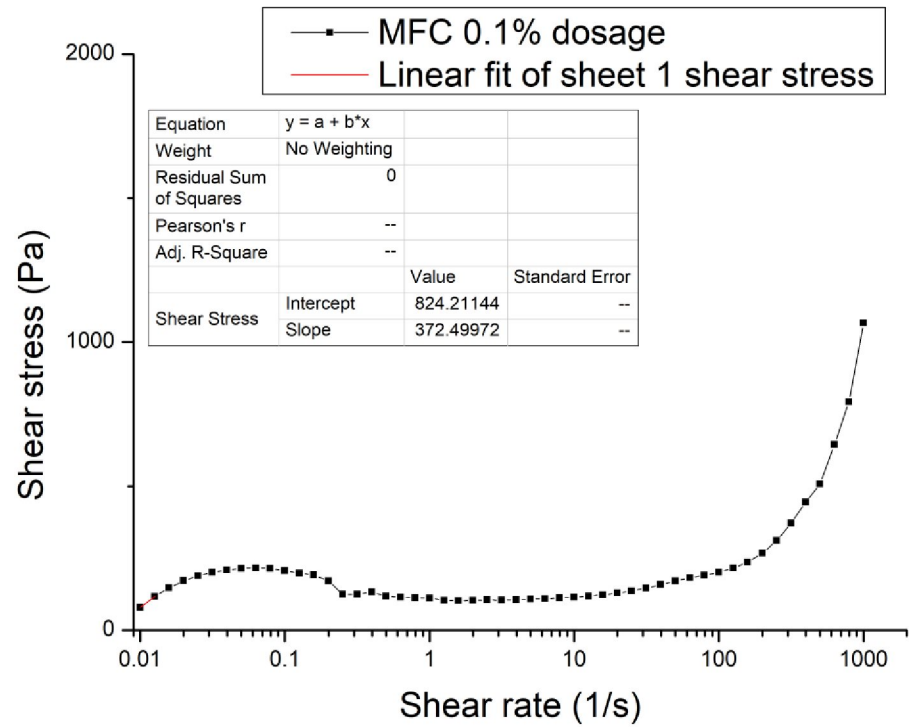
Figure 38. Shear stress vs shear rate curve for MFC 0.1%.
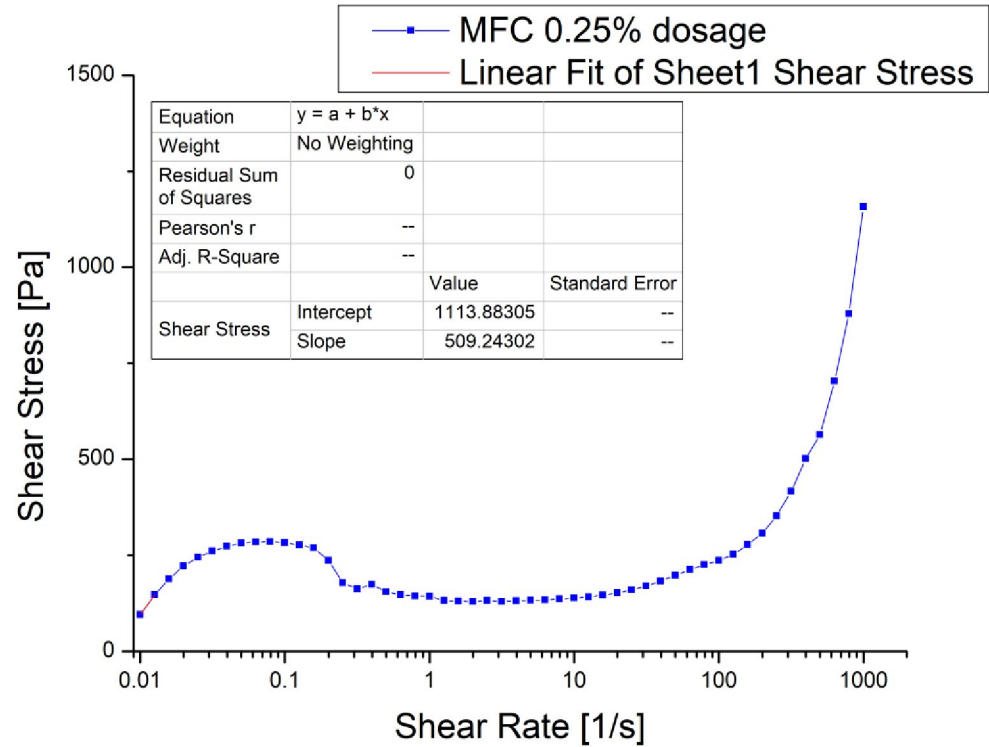
Figure 39. Shear stress vs shear rate curve for MFC 0.25%.
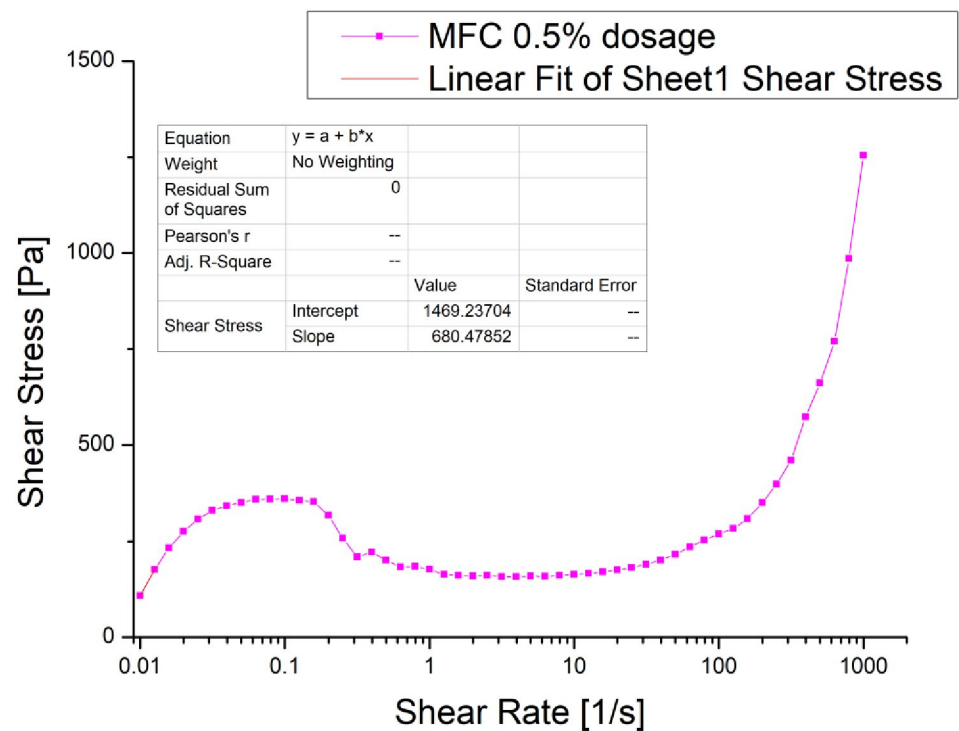
Figure 40. Shear stress vs shear rate curve for MFC 0.5%.
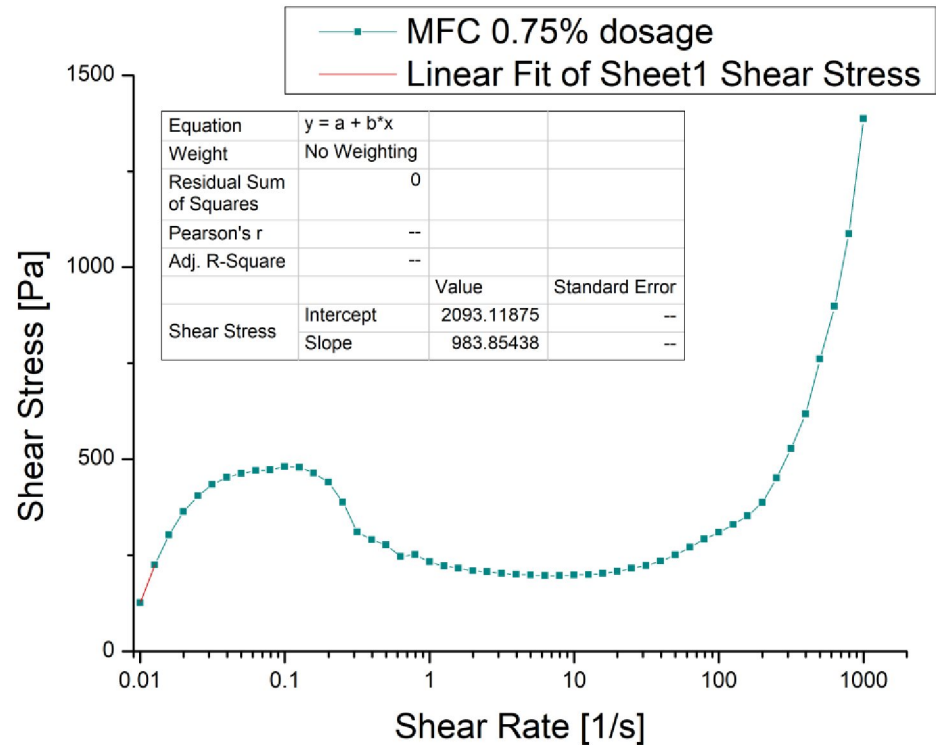
Figure 41. Shear stress vs shear rate curve for MFC 0.75%
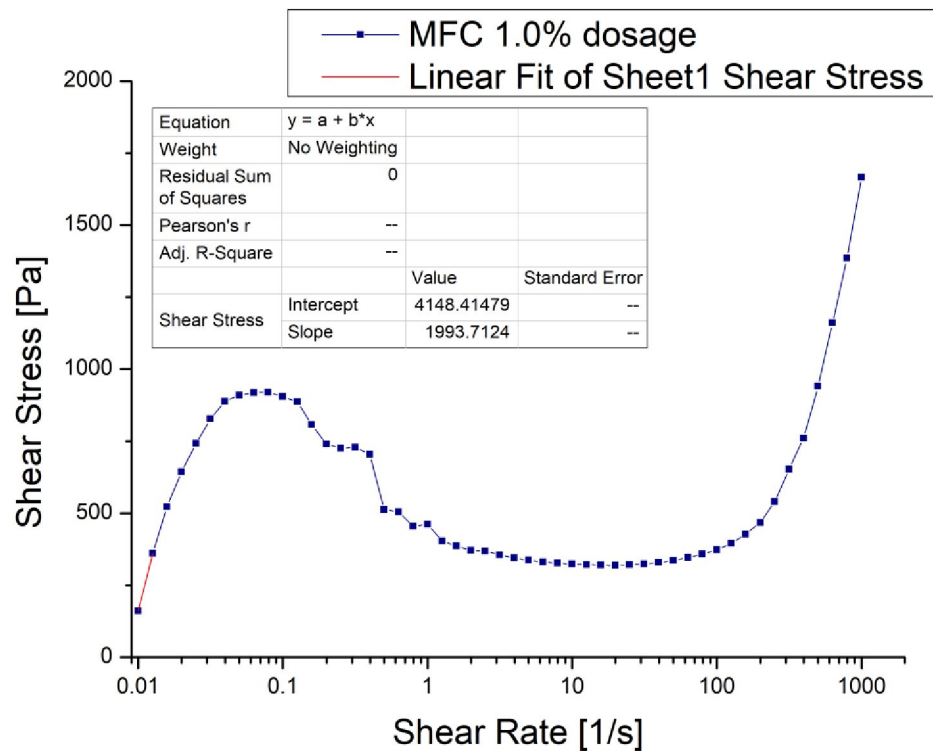
Figure 42. Shear stress vs shear rate curve for MFC 1.0%.

The values for dynamic yield stress and plastic viscosity are therefore measured through the respective graphs with results tabulated below in table (10). The net relationship between all curves is also presented in fig. (43).

Table 10. Overview of the dynamic yield stress and plastic viscosity values.

Mix-design	Dynamic yield stress (Pa)	Plastic viscosity (Pa. s)
Control reference	804.23	372.4
MFC 0.1%	824.21	372.5
MFC 0.25%	1113.88	509.24
MFC 0.5%	1469.23	680.47
MFC 0.75%	2093.11	983.85
MFC 1.0%	4148.4	1993.71
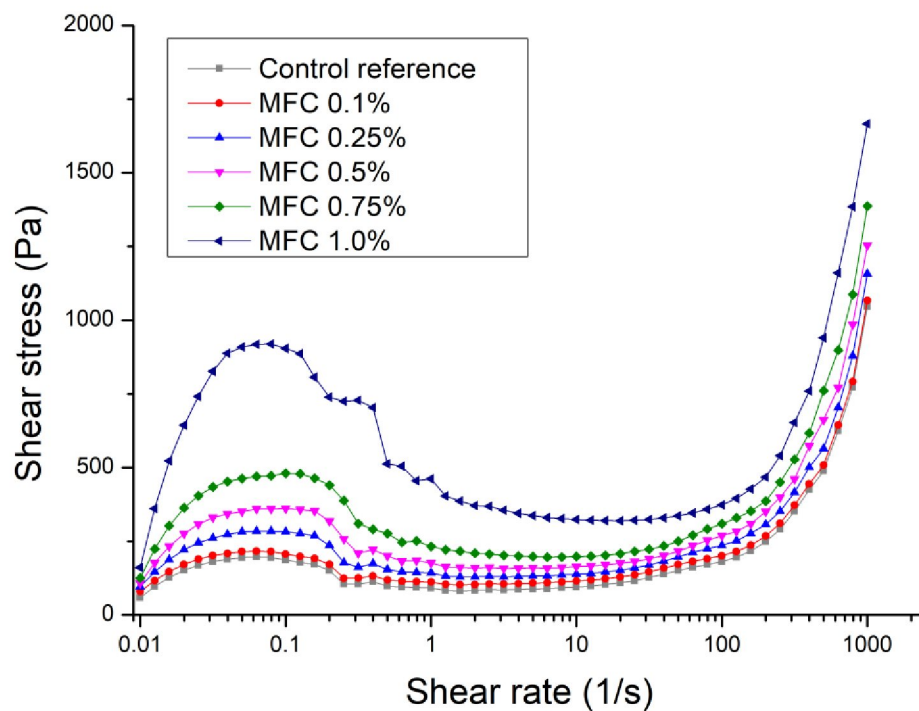
Figure 43. Shear stress vs shear rate comparison between all shotcrete pastes.

As shown in fig. (44), despite the negligible difference between control reference and MFC 0.1% concentration, the overall trend highlights the increment in dynamic yield stress and plastic viscosity in a directly proportional manner, with the increase in dosage of MFC. There seems to be dramatic rise in dynamic yield stress at a dosage value of 1%, indicating that the paste was too viscous. These results show that the addition of MFC serves to raise the plastic viscosity of the shotcrete mix-design when compared with control reference pastes. From the trend in fig. (44), it can be suggested that the dosage values from 0.25% to 0.75% MFC are most favourable in terms of reducing rebound.
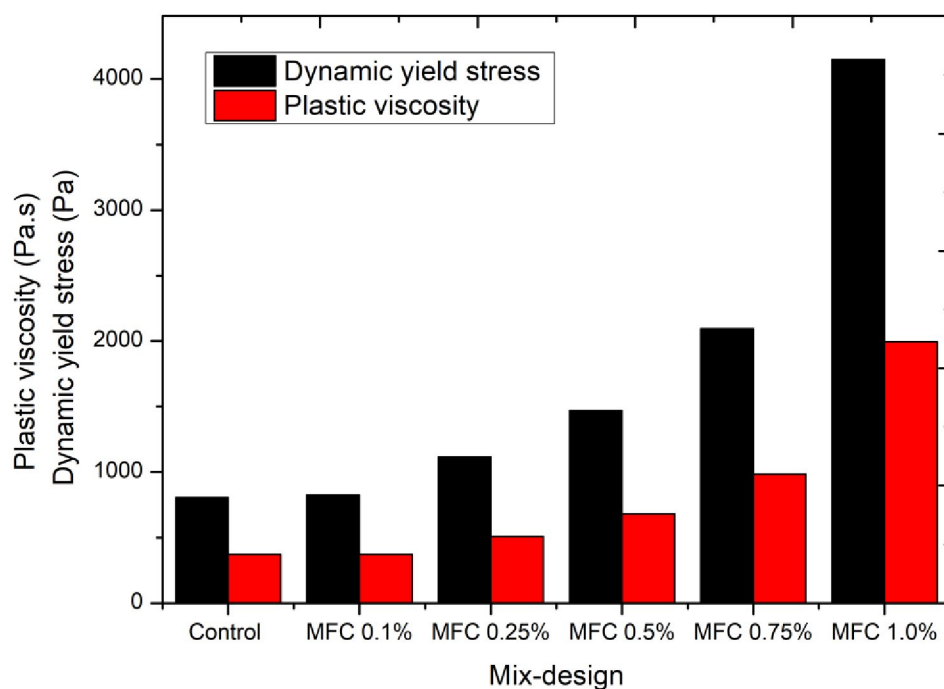
Figure 44. Comparison between dynamic viscosity and plastic viscosity for the mix.

6.3   Isothermal calorimetry

Isothermal calorimetric tests were performed to obtain an insight into the early-stage hydration reactions, setting behavior, and overall heat release of all the shotcrete cementitious paste mix-designs. Following procedure was adopted: (1) sample preparation, (2) setting up the calorimeter, (3) setting up the bath temperature, (4) placing the samples in the calorimeter, and (5) running the test [49].

The test duration was set to run for 07 days to allow enough time to capture and analyze the heat evolution and hydration response of the cementitious material during the early stages of its curing process [49]. Table (11) presents the mass of each sample utilized in this test. At the end of 07 days, the sample vials were removed, and the data was collected and observed in TAM and Cement Analysis software.

Table 11. Cementitious sample vial mass placed in the TAM calorimeter.

Sample	Mass (g)
Control reference	5.529
MFC 0.1%	5.637
MFC 0.25%	5.507

MFC 0.5%	5.425
MFC 0.75%	5.391
MFC 1.0%	5.702

6.3.1   Cement hydration curves

Through the hydration curves, Peak and Kinetic Analyses were conducted to determine the maximum rate of heat release, and kinetics of the hydration process. This data also provided details regarding the setting time. Fig. (45), (46), (47), (48), (49) and (50) illustrate the hydration curves for the shotcrete cementitious hydration curves.
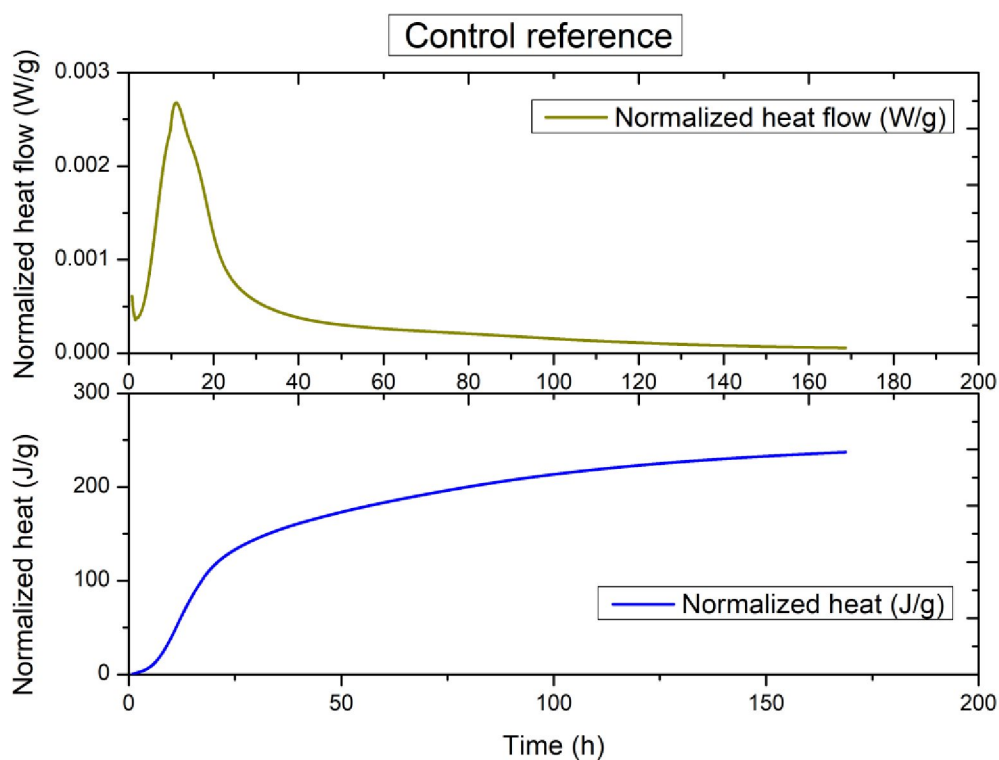
Figure 45. Hydration curve for shotcrete control reference sample.
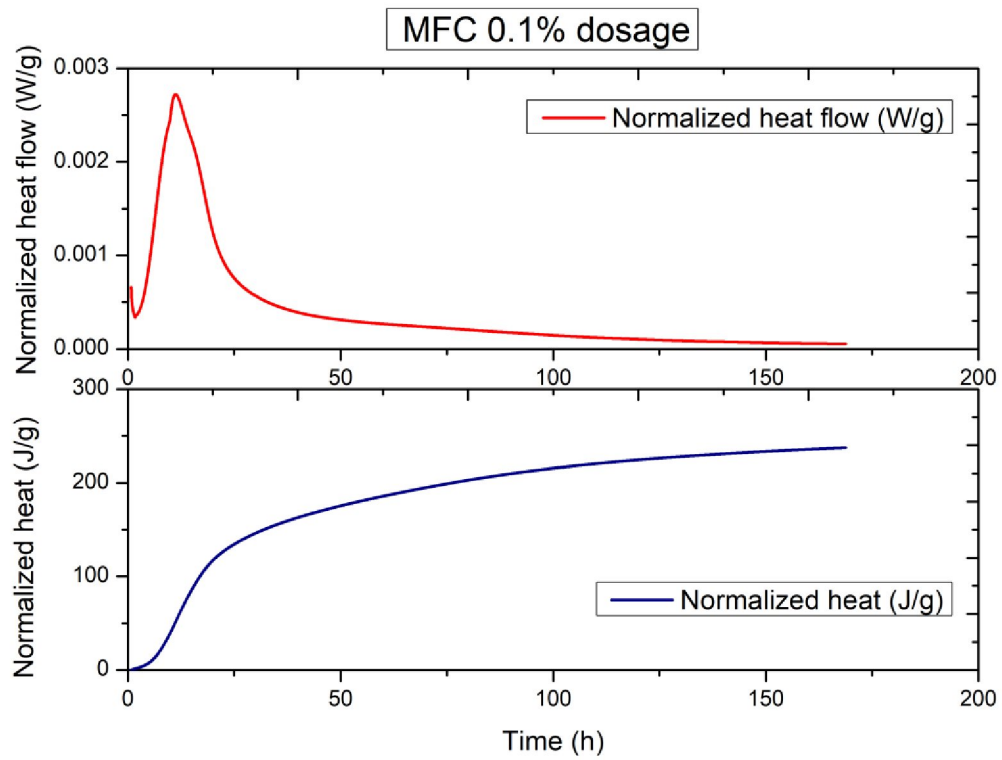
Figure 46. Hydration curve for shotcrete MFC 0.1% sample.
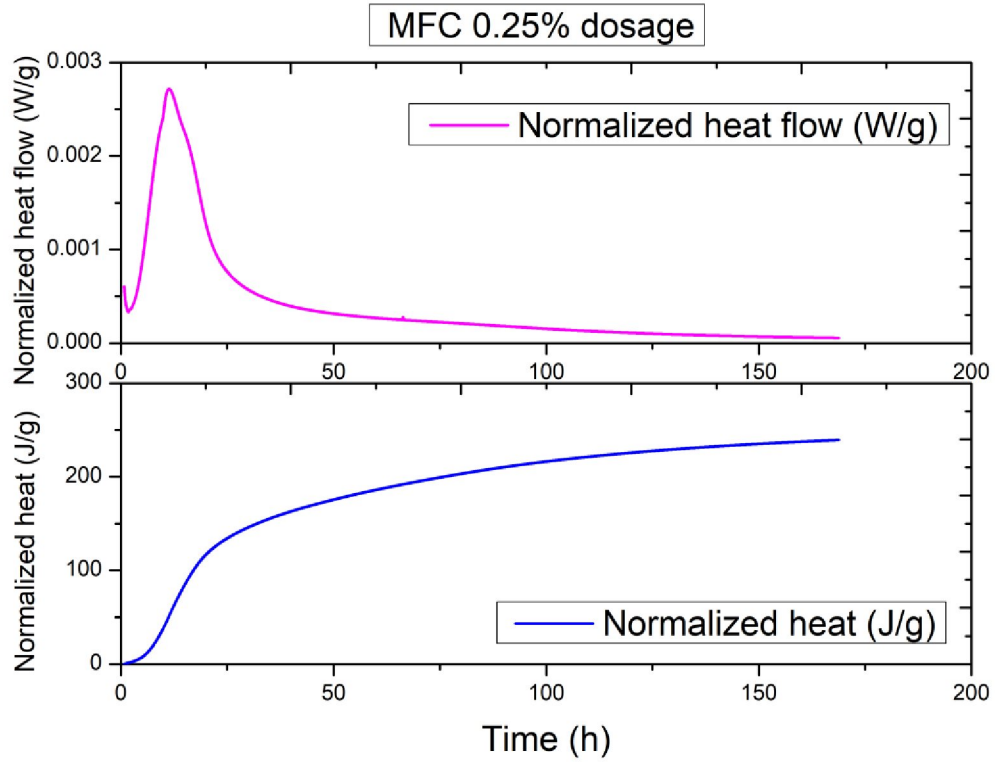
Figure 47. Hydration curve for shotcrete MFC 0.25% sample.
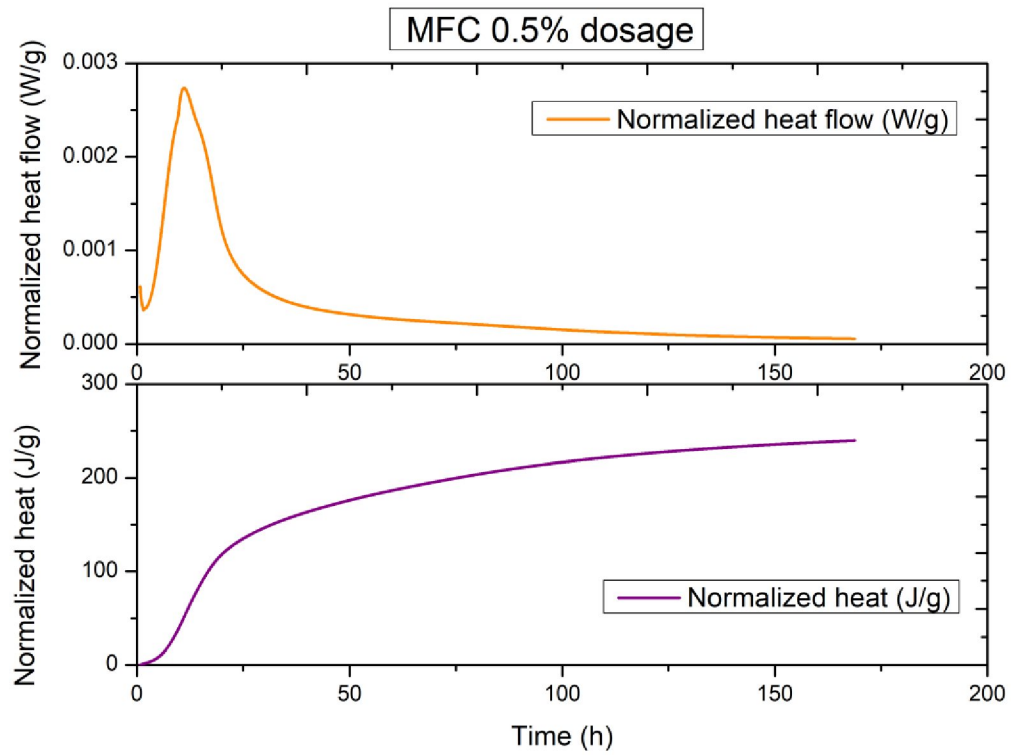
Figure 48. Hydration curve for shotcrete MFC 0.5% sample.
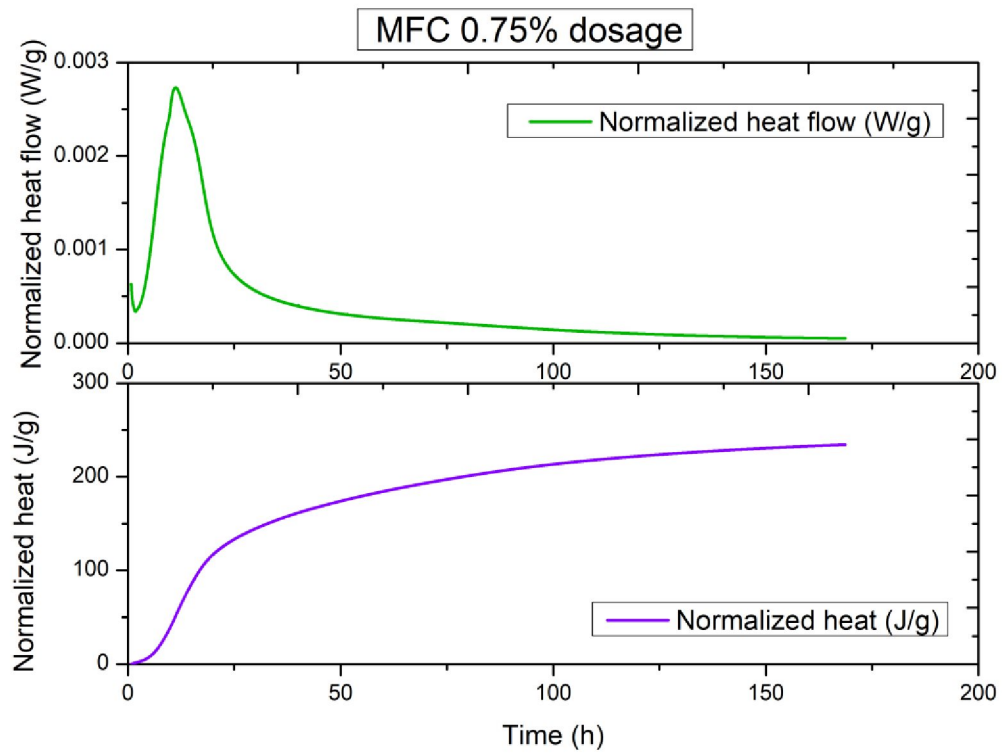
Figure 49. Hydration curve for shotcrete MFC 0.75% sample.
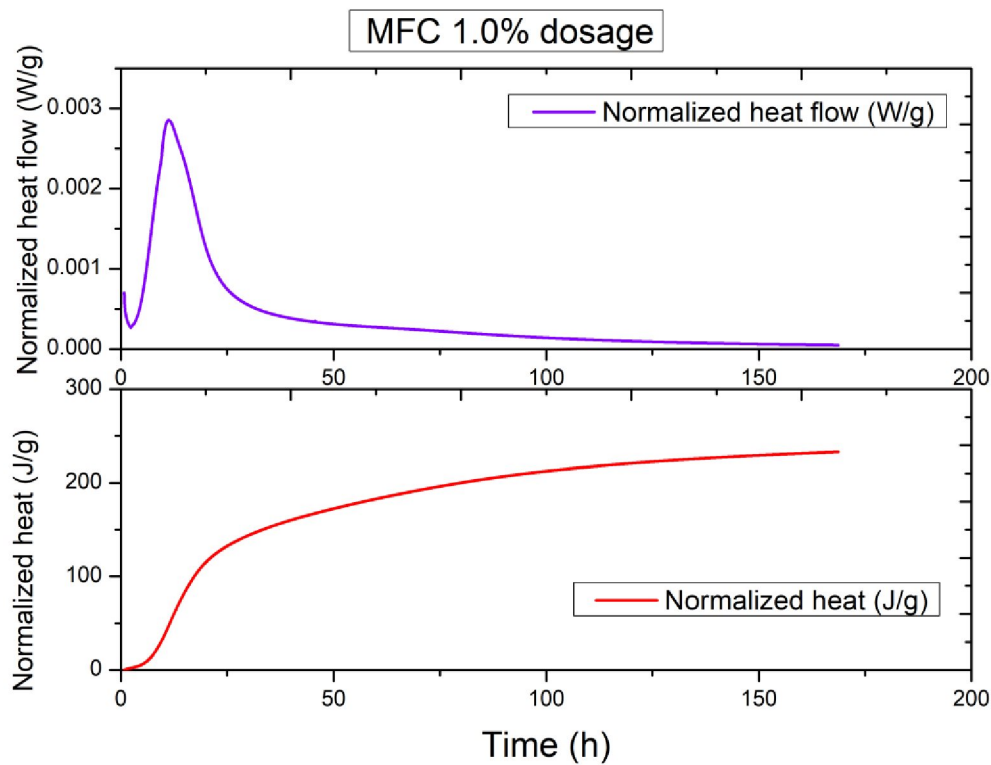
Figure 50. Hydration curve for shotcrete MFC 0.1% sample.

Using TAM Assistant tool and Cement Analysis software, these hydration curves provided detailed insight into the kinetics and progress of cement hydration under different concentration of MFC. These curves are presented in from of 'Normalized heat flow vs time' and 'Normalized heat vs time' curves. Using the normalized heat flow curve, the rate of heat release was calculated, while normalized heat curve provided a cumulative total of heat released or absorbed over time. Plotting these curves together allows for additional comparison between the test samples, as shown in fig. (51). Data corresponding to the important points on the hydration curve were extracted from the Cement Analysis software, as summarized in table (12).
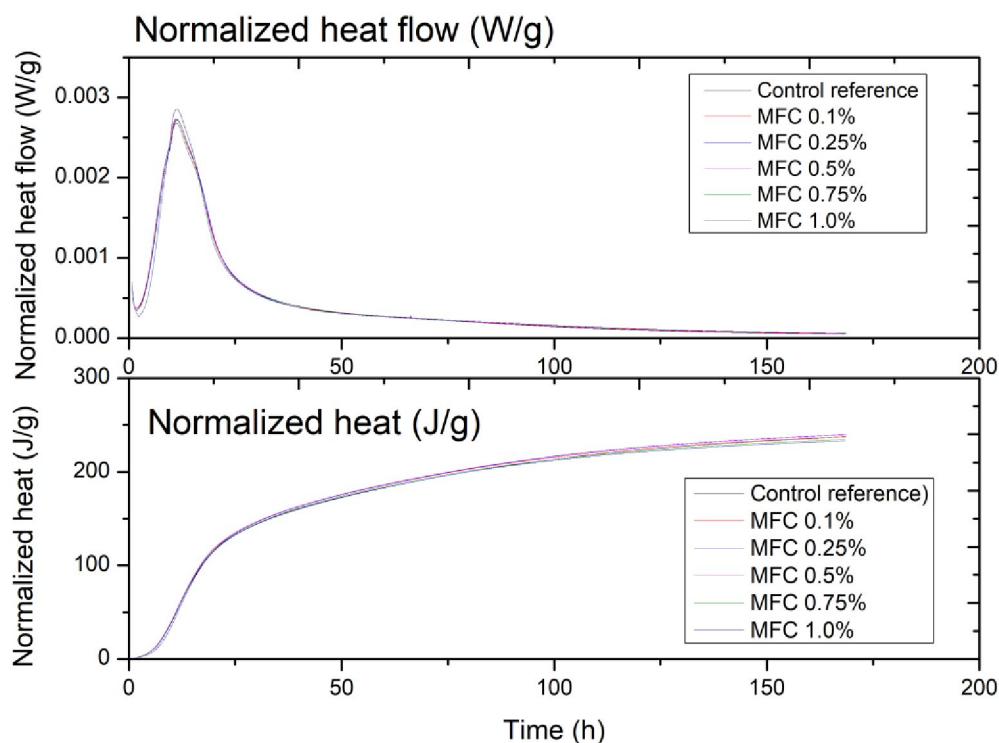
Figure 51. Net comparison of hydration curves between control and MFC samples.

Table 12. Isothermal calorimetry results for cement hydration conducted at Østfold University College laboratory.

Cementitious sample	Heat after 1 hour	Heat after 1 day	Heat after 3 days	Heat after 7 days	Time to peak	Peak max	Time to initial set point	Time to final set point
	J	J	J	J	hr	W	hr	hr
Control	0.0098436	712.6	1065	1303.7	11.15	0.014802	5.1	8.46
MFC 0.1%	0.0080051	616.65	924.43	1116.8	11.21	0.012884	5.06	8.4
MFC 0.25%	0.008653	674.4	1014.3	1234.5	11.33	0.014099	5.19	8.56
MFC 0.5%	0.0098639	721.71	1079.3	1311.5	11.12	0.015059	5.02	8.36
MFC 0.75%	0.0090721	694.46	1041.9	1254.3	11.2	0.014715	5.11	8.45
MFC 1.0%	0.0070414	673.22	1011.5	1216.9	11.28	0.015055	5.76	9.03

6.3.2   Heat release pattern

As evident from table (12), the control sample exhibits consistently higher heat release levels across the test time interval. In contrast, the heat release was found to decrease as the MFC percentage increases, indicating a potential influence on the additive on hydration kinetics.

6.3.3   Time to peak hydration

Time to peak heat release remained remarkably consistent around 11.2 hours for all samples, suggesting a consistent rate of maximum hydration activity, regardless of the presence of MFC, as evident from table (12).

6.3.4   Peak heat release

As seen from table (12), the control and MFC 0.5% samples demonstrate the highest peak heat release, while MFC 1.0% shows a slightly lower peak. Peak heat release rates follow a similar trend, indicating a moderate effect on hydration kinetic via MFC.

6.3.5   Setting time

The initial and final set points demonstrate minimal deviations across all samples, as recorded in table (12). This consistency in setting times indicate that the introduction of MFC does not significantly alter the early stages of hydration.

Overall, the introduction of MFC additive appears to have a minor influence on heat release, especially at higher percentages. However, the effect on setting times and time to peak remains relatively consistent.

7 Discussion on test results

7.1 Flow table tests

Results from the flow table tests (as presented in chapter 5.1) exhibit decrement in slump height and flow up to a dosage of 0.75% MFC, a trend indicative of decreased workability compared to the reference control mix, owing to the development of more viscous mix with increase in MFC concentration. However, beyond 0.75% dosage, a sudden rise in slump height and flow was observed at 1.0% MFC, which could be attributed to poor mixing in the mix-design due to increased viscosity at this value of MFC concentration.

7.2 Air content

The air content results presented in fig. (31) showed minor variation across all mix-designs with a standard deviation of around 0.28 with reference to the control mix. This affirms that MFC has minor impact as an air entraining admixture and could be viewed as a favourable outcome for improved freeze-thaw resistance. Detailed study into the spacing factor and distribution of air voids within the mixture would require analysis of thin sections with polarization microscope, which falls out of the scope of this dissertation.

7.3 Mechanical strength development

Investigation into compressive and flexural strength (MPa) exhibited a small increment in these mechanical properties in a gradual manner up to its complete strength development after 28 days, with the highest strength values recorded of MFC dosage at 0.75%. It was also noticed at beyond a dosage of 0.75%, there was a decrement in both compressive and flexural strength compared to control reference mix. This behavior can be attributed to the visible increment in viscosity with MFC mix, thus not allowing for proper mixing.

7.4 Setting time

As deduced from fig. (34) and (35), there is no significant impact on the setting times with the addition of MFC compared with the control reference sample, indicating that the mix-design remains consistent with the addition of Microfibrillated cellulose admixture.

7.5 Rheology

Results from the rheological analyses (chapter 6.2), indicate that there was in increase in the static yield stress in a proportional manner with the increasing dosage of MFC.

Similarly, a linear increment was observed in the dynamic yield strength and plastic viscosity, with increasing concentration of MFC. This indicates a good potential for spray application initiation, as addition of MFC would render the shotcrete being less likely to start flowing on its own through the nozzle, thus providing stability and preventing premature loss of material with good pumpability, and this also serves as a good potential to mitigate the rebound effect. However, a conduction of a formal spray test for the control and MFC samples would give additional insight.

7.6   Heat of hydration

As analysed from chapter 6.3, the isothermal calorimetry of all shotcrete paste mix designs revealed minor variation in the hydration kinetics, and on the overall hydration process. Overall, the introduction of MFC additive appears to have a minor influence on heat release, especially at higher percentages. However, the effect on setting times and time to peak remains relatively consistent. This indicates that the overall exothermic reaction of cement hydration remains largely stable, even with the introduction of MFC admixture. Therefore, while the addition of MFC may subtly influence the heat generation process, its influence on the crucial stages of setting and reaching peak hydration activity remains relatively uniform when compared with the control reference sample.

8   Conclusion

The effect of 10% paste solution Microfibrillated Cellulose (MFC) on the physical, mechanical, flow and chemical properties of shotcrete has been studied. Different concentrations of MFC in terms of solids by weight of binder (sbwb) within the mix-design were prepared and investigated against the reference base sample. In order to achieve comparable data, all samples preparation and experiments were carried out under identical conditions.

The investigation into the development of MFC based shotcrete mix-design reveal the following observations:

  i.   Microfibrillated Cellulose (MFC) acts as a viscosity modifying admixture (VMA) in the shotcrete mix-design, with observed reduction in slump height and flow properties. This reduces the workability of shotcrete however the values are within range to exhibit good workability for flow application.

 ii.   There was no adverse impact on the 28-day compressive and flexural strength or the air content of the tested mix-designs. MFC exhibits a minor accelerating effect on the initial setting time with a slight delaying effect on the final setting time.

iii.   Rheological analysis determined that MFC contributes to the increment in the static and dynamic yield stress as well as the plastic viscosity of the mix-design in a linear progression with increasing dosage. This observation holds good potential for reducing rebound effect.

 iv.   There is no adverse effect on the hydration kinetics of the shotcrete mix-design with the inclusion of MFC, indicating that it does not interfere with the essential setting and hardening reaction of the shotcrete mix.

In line with the pursuit of sustainable construction practices, this study revealed the potential posed by Microfibrillated Cellulose in improving or maintaining standard shotcrete properties while its nature as a bio-based admixture resonates with the industrial efforts to embrace environmentally friendly alternative that enhances both performance and eco-consciousness.

9   Future work

In extension to the mechanical, physical, rheological and chemical property testing of the shotcrete mix-designs, an approach to design shotcrete spray tests are underway, with the development of a lab scale shotcrete spray gun as shown in fig. (52). These spray tests would aid in deducing the rebound reduction potential and source for comparison with the results obtained from the flow table tests and rheology analyses. The spray tests will be conducted between August and September 2023.

Figure 52. Lab scale shotcrete spray gun assembled at Østfold University College.

Additional test with a different batch of Microfibrillated Cellulose as a 2% solution (2% fibrils, 98% water) were also performed. However their results were not a part of this dissertation. It its recommended to conduct a comparison analysis between the two MFC batches for better understanding and insight of cellulose impact on shotcrete.

Another recommendation for detailed economic evaluation and insight into approaching sustainablity would be to perform a Life Cycle Assessment (LCA) for the shotcrete mix-design with MFC and comparing it with the control sample.

References

1.   Mohajerani, A., et al., *Early-Age Strength Measurement of Shotcrete.* Journal of Materials, 2015. **2015**: p. 470160.

2.   Bernard, E.S., *Early-age load resistance of fibre reinforced shotcrete linings.* Tunnelling and Underground Space Technology, 2008. **23**(4): p. 451-460.

3.   Zhang, L.J., *Is shotcrete sustainable?* . 2010, American Shotcrete Association. p. 7.

4.   Hasanbeigi, A., L. Price, and E. Lin, *Emerging energy-efficiency and CO2 emission-reduction technologies for cement and concrete production: A technical review.* Renewable and Sustainable Energy Reviews, 2012. **16**: p. 6220–6238.

5.   Ezgi Yurdakul, K.-A.R., and Diego Granell Nebot, *An Approach for Improving the Sustainability of Shotcrete.* . Sustainability, 2016.

6.   Benedikt Lindlar, M.J., Jürg Schlumpf, *SIKA Sprayed Concrete Handbook.* 2020.

7.   Teirfolk, J.-E., et al., *Nanosized cellulose fibrils.* Concrete Plant International, 2012. **6**: p. 46-49.

8.   Burak, E., Y. Vorob'eva, and R. Sheps, *Investigation of the Strength Characteristics of Shotcrete as a Function of the Technological Parameters of the Application.* IOP Conference Series: Materials Science and Engineering, 2018. **463**: p. 042015.

9.   Gandage, A., *Admixtures in Concrete -A Review.* 2023.

10.   Beaupre, D., *Rheology of high performance shotcrete* 1994, University of Laval; Department of Civil Engineering.

11.   Khitab, A., *Shotcrete: Methods and Compositions.* 2015.

12.   Ginouse, N. and S. Reny, *RAPID FLEXURAL TOUGHNESS DEVELOPMENT DRY-MIX SHOTCRETE FOR MINING APPLICATIONS.* 2015.

13.   Pan, G., et al., *A study of the effect of rheological properties of fresh concrete on shotcrete-rebound based on different additive components.* Construction and Building Materials, 2019. **224**: p. 1069-1080.

14.   Yun, K.K., S.-Y. Choi, and J.H. Yeon, *Effects of admixtures on the rheological properties of high-performance wet-mix shotcrete mixtures.* Construction and Building Materials, 2015. **78**.

15.   Pan, G., et al., *A study of the effect of rheological properties of fresh concrete on shotcrete-rebound based on different additive components.* Construction and Building Materials, 2019. **224**.

16.   Sika, *Sika® ViscoCrete®-4028 SC SUPER PLASTICISING ADDITIVES FOR INJECTED CONCRETE*, S. Norway, Editor. 2023.

17.   Liu, Z., et al., *Influences on Shotcrete Rebound from Walls with Random Roughness.* Advances in Materials Science and Engineering, 2018. **2018**: p. 1-12.

18.   Lam, T., et al., *The Properties of High-strength Concrete with High Volume of Natural Pozzolan.* IOP Conference Series: Materials Science and Engineering, 2020. **869**: p. 032023.

19.   Talaat, A., et al., *Factors affecting the results of concrete compression testing: A review.* Ain Shams Engineering Journal, 2021. **12**(1): p. 205-221.

20.   Sutar, S., et al., *Study and Review of Ordinary Portland Cement.* ASEAN Journal of Science and Engineering, 2021. **1**: p. 153-160.

21.   Ali, I.A. Khan, and M.I. Hossain, *CHEMICAL ANALYSIS OF ORDINARY PORTLAND CEMENT OF BANGLADESH.* Chemical Engineering Research Bulletin, 2008. **12**: p. 7-10.

22.   CEMENT, A.R., *Aalborg RAPID® cement CEM I 52,5 N (LA).* 2022.

23.   Rajendran, S., *Silica fume as Partial Replacement of Cement in Concrete.* International Research Journal of Multidisciplinary Technovation, 2019. **1**: p. 325-333.

24.   ELKERM, *Elkem Microsilica® 920D Concrete applications – Product data sheet.* 2017, Elkem Microsilica®.

25.   Mogre, R., D. Parbat, and S. Bajad, *Feasibility Of Artificial Sand In Concrete.* International Journal of Engineering Research & Technology (IJERT) Vol. 2 Issue 7, July - 2013 IJERTIJERT ISSN: 2278-0181, 2013. **2**: p. 1607-1610.

26.   Sze, A., et al., *Sand Properties for Concrete Application.* 2021.

27.   International, A., *ASTM D2216-19 (2019). Standard Test Methods for Laboratory Determination of Water (Moisture) Content of Soil and Rock by Mass.* 2019, American Society for Testing and Materials: West Conshohocken, PA.

28.   Martin, J.W., *Materials for Engineering (Third Edition).* 2006.

29.   Salem, M., S. Alsadey, and M.A. Megat Johari, *Effect of Superplasticizer Dosage on Workability and Strength Characteristics of Concrete.* IOSR Journal of Mechanical and Civil Engineering, 2016. **13**: p. 153-158.

30.   Klemm, D., et al., *Nanocelluloses: A New Family of Nature-Based Materials.* Angewandte Chemie (International ed. in English), 2011. **50**: p. 5438-66.

31.   Teirfolk, J.-E., et al. *NANOSIZED CELLULOSE FIBRILS– A NEW GENERATION STABILIZER FOR CONCRETE AND GROUTS.* 2012.

32.   Al-Jabri, K.S., et al., *Effect of using Wastewater on the Properties of High Strength Concrete.* Procedia Engineering, 2011. **14**: p. 370-376.

33.   Li, W., *Analysis of the Influence of Water-cement Ratio on Concrete Strength.* E3S Web of Conferences, 2021. **283**: p. 01016.

34.   Akinwumi, I. and Z. Gbadamosi, *Effects of Curing Condition and Curing Period on the Compressive Strength Development of Plain Concrete.* International Journal of Civil and Environmental Research, 2014. **1**: p. 83-99.

35.   Kimsan, M., et al., *Temperature Evaluation of Stage Method of Mass Concrete Construction in Determining Direct Method Strategy.* 2015.

36.   Pawar, Y. and S. Kate, *Curing of Concrete: A Review.* 2020.

37.   Bernardo, G., A. Guida, and I. Mecca. *Advancements in shotcrete technology.* WIT Press.

38.   Materials, A.S.f.T.a., *Standard Test Method forSlump of Hydraulic-Cement Concrete.* 2020. **C143/C143M−20**: p. 4.

39.   NS-EN, *Testing fresh concrete - Part 5: Flow table test.* 2019.

40.   ASTM, *Standard Test Method for Flow of Hydraulic Cement Mortar.* 2020.

41.   NS-EN, *Methods of test for mortar for masonry - Part 7: Determination of air content of fresh mortar*. 1998, NS-EN 1015-7:1998.

42.   Bagherzadeh, R., et al., *An Investigation on Adding Polypropylene Fibers to Reinforce Lightweight Cement Composites (LWC)*. Journal of engineered fibers and fabrics, 2012. **7**: p. 13-21.

43.   Vila, P., M.N. Pereyra, and Á. Gutiérrez. *Compressive strength in concrete paving blocks. Results leading to validate the test in half-unit specimens*. 2017.

44.   Wang, L., et al., *Mechanical properties of dental restorative materials: Relative contribution of laboratory tests*. Journal of applied oral science : revista FOB, 2003. **11**: p. 162-7.

45.   (ASTM), A.S.f.T.a.M., *Standard Test Method for Compressive Strength of Hydraulic-Cement Mortars*. 2021, ASTM. p. 4.

46.   Amziane, S., *Setting time determination of cementitious materials based on measurements of the hydraulic pressure variations*. Cement and Concrete Research, 2006. **36**: p. 295-304.

47.   Jiao, D., et al., *Effect of constituents on rheological properties of fresh concrete-A review*. Cement and Concrete Composites, 2017. **83**: p. 146-159.

48.   Kolawole, J.T., R. Combrinck, and W.P. Boshoff, *Rheo-viscoelastic behaviour of fresh cement-based materials: Cement paste, mortar and concrete*. Construction and Building Materials, 2020. **248**: p. 118667.

49.   Wadsö, L., *Applications of an eight-channel isothermal conduction calorimeter for cement hydration studies*. Cement International, 2005. **5**: p. 94-101.

50.   Lars Wadsö, F.W., Kyle Riding and Paul Sandberg, *Practical Guide to Microstructural Analysis of Cementitious Materials*. 2017.

Appendix

A.1. Nomenclature

MFC	Microfibrillated Cellulose
VMA	Viscosity Modifying Admixture
OPC	Ordinary Portland Cement
TAM	Thermometric Analysis Module
HPWMS	High performance wet-mix shotcrete
AEA	Air Entraining Admixture
Sbwb	Solids by weight of binder
sbwc	Solids by weight of cement
UTM	Universal Testing Machine
ASTM	American Society for Testing and Materials
EN	European Standards
SEM	Scanning Electron Microscope
SF	Silica Fume
SP	Super Plasticizer

A.2. Symbols

w/c	Water-to-cement ratio
w/b	Water-to-binder ratio
R	Rebound
m	Mass of material lost as rebound
M	Total mass of sprayed shotcrete
f	Mean value of slump flow
d	Maximum diameter of slump
Fc	Compressive strength
P	Applied load

A   Cross section area of mortar

Ff   Flexural strength

τ Shear stress

τo Dynamic yield stress

μ   Plastic viscosity

γ Shear rate

A.3.   Experimental results for chapter 5

A.3.1   Flow-table tests and air content test

Tests	Ref.	Exilva P 01-V 0.1%	Exilva P 01-V 0.25%	Exilva P 01-V 0.5%	Exilva P 01-V 0.75%	Exilva P 01-V 1%
Slump Height (mm)	87	80	62	60	50	87.5
Flow (mm)	478	450	425	395	360	436.5
Mini-Slump (mm)	133	130	125	120	110	125
Air Content (%)	6.0	6.2	6.4	6.6	6.6	6.8

A.3.2.   Compressive strength

	Compressive strength (Mpa)		
Mix design	24 h	D 07	D 28
Control	47.14667	61.8	72.43333
MFC 0.1%	46.84	55.49333	67.30667
MFC 0.25%	34.41333	64.93333	73.72
MFC 0.5%	33.26667	60.72	71.42667
MFC 0.75%	39.26667	65.76	80.13333
MFC 1%	25.90667	57.57333	67.58667

A.3.4.   Flexural strength

	Flexural strength (MPa)		
Mix design	24 h	D 07	D 28
Control	3.95617	5.52625	7.30195
MFC 0.1%	4.09148	4.56719	6.42828
MFC 0.25%	4.68797	5.57086	7.1343
MFC 0.5%	4.59094	5.36305	7.01258
MFC 0.75%	4.92289	5.73453	7.97078
MFC 1%	4.20914	4.14063	5.68

A.4.   Experimental results from chapter 6

A.4.1. Setting time tests

A.4.1.1.   Control

CERTIFICATE

TEST NUMBER : 01CT	DATE OF TEST : 26/07/2023	FINAL SETTING : NO
KIND OF TEST : EN196-3:2005	SPECIMEN TIME : 14:00:52	TIME [m] : 5
POINTS MOVE [mm]	START DELAY[m]: ---	
30 4.00	1ST PEN TIME : 14:27:52	
24 5.25	SPECIMEN TYPE : C1	
18 5.25	WATER CONT.[%]: 40.0	
12 5.25	TEMPERATUR[øC]: 22.8	
2 5.25	HUMIDITY[%] : 46.4	
OPERATOR CODE : FKA	FALL TYPE : FREE	
CUSTOMER CODE : CEM1	TIME TYPE : FIXED	
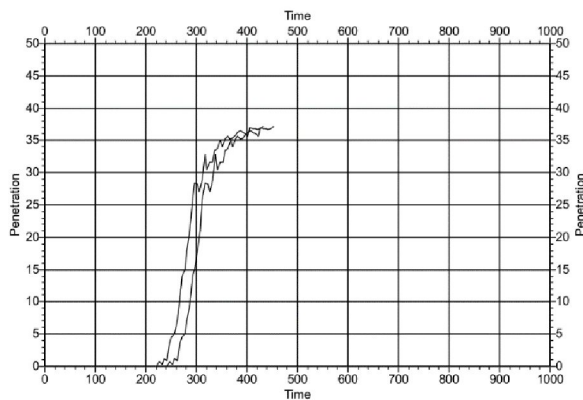
A.4.1.2.   MFC 0.1%

CERTIFICATE

TEST NUMBER : 02EV01   DATE OF TEST : 27/07/2023   FINAL SETTING : NO

KIND OF TEST : EN196-3:2005   SPECIMEN TIME : 11:13:06   TIME [m]   : 5

POINTS MOVE [mm]   START DELAY[m]: ---

  30   4.00   1ST PEN TIME : 11:46:06

  24   5.25   SPECIMEN TYPE : C1

  18   5.25   WATER CONT.[%]: 40.0

  12   5.25   TEMPERATUR[øC]: 23.1

   2   5.25   HUMIDITY[%]   : 46.0

OPERATOR CODE : FKA   FALL TYPE   : FREE

CUSTOMER CODE : CEM1   TIME TYPE   : FIXED

A.4.1.3.   MFC 0.25%

CERTIFICATE

TEST NUMBER   : 03EV025   DATE OF TEST : 28/07/2023   FINAL SETTING : NO

KIND OF TEST : EN196-3:2005   SPECIMEN TIME : 10:15:05   TIME [m]   : 10

POINTS MOVE [mm]   START DELAY[m]: ---

  30   4.00   1ST PEN TIME : 10:53:05

  24   5.25   SPECIMEN TYPE : C1

  18   5.25   WATER CONT.[%]: 40.0

  12   5.25   TEMPERATUR[øC]: 23.1

   2   5.25   HUMIDITY[%] : 55.8

OPERATOR CODE : FKA   FALL TYPE   : FREE
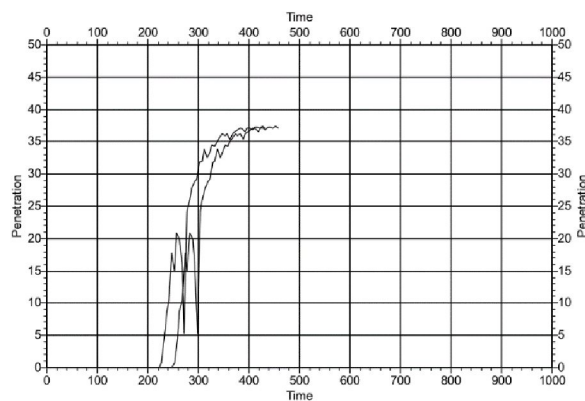
CUSTOMER CODE : CEM1   TIME TYPE   : FIXED

A.4.1.4.   MFC 0.5%

CERTIFICATE

TEST NUMBER   : 04EV05   DATE OF TEST : 31/07/2023   FINAL SETTING : NO
KIND OF TEST : EN196-3:2005   SPECIMEN TIME : 11:47:32   TIME [m]   : 10
POINTS MOVE [mm]   START DELAY[m]: ---
    30   4.00   1ST PEN TIME : 12:15:32
    24   5.25   SPECIMEN TYPE : C1
    18   5.25   WATER CONT.[%]: 40.0
    12   5.25   TEMPERATUR[øC]: 23.0
     2   5.25   HUMIDITY[%]   : 50.6
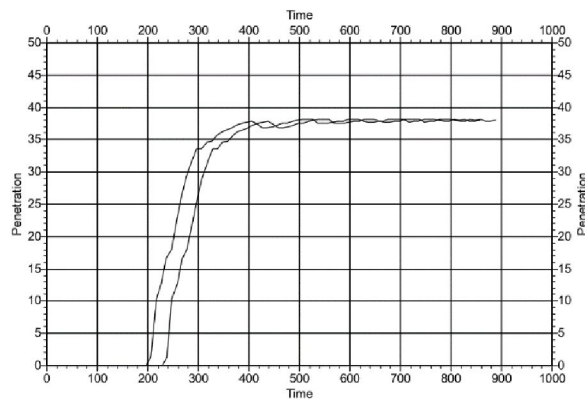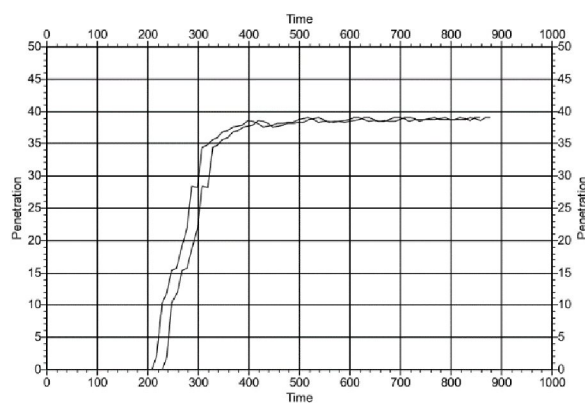OPERATOR CODE : FKA   FALL TYPE   : FREE
CUSTOMER CODE : CEM1   TIME TYPE   : FIXED

A.4.1.5. MFC 0.75%

CERTIFICATE

TEST NUMBER : 05EV075	DATE OF TEST : 01/08/2023	FINAL SETTING : NO
KIND OF TEST : EN196-3:2005	SPECIMEN TIME : 09:14:33	TIME [m] : 10
POINTS MOVE [mm]	START DELAY[m]: ---	
30 4.00	1ST PEN TIME : 09:47:33	
24 5.25	SPECIMEN TYPE : C1	
18 5.25	WATER CONT.[%]: 40.0	
12 5.25	TEMPERATUR[øC]: 23.0	
2 5.25	HUMIDITY[%] : 51.8	
OPERATOR CODE : FKA	FALL TYPE : FREE	
CUSTOMER CODE : CEM1	TIME TYPE : FIXED	

A.4.1.6.   MFC 1.0%

CERTIFICATE

KIND OF TEST : EN196-3:2005   SPECIMEN TIME : 12:38:00   TIME [m]   : 10

POINTS MOVE [mm]   START DELAY[m]: ---

  30   4.00   1ST PEN TIME : 13:22:56

  24   5.25   SPECIMEN TYPE : C2

  18   5.25   WATER CONT.[%]: 40.0

  12   5.25   TEMPERATUR[øC]: 22.5

   2   5.25   HUMIDITY[%]   : 19.1

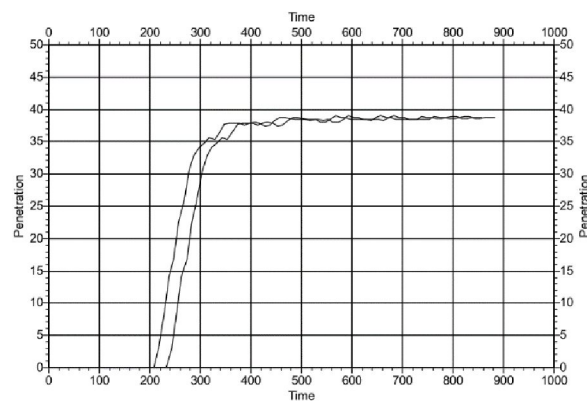OPERATOR CODE : FAR   FALL TYPE   : FREE

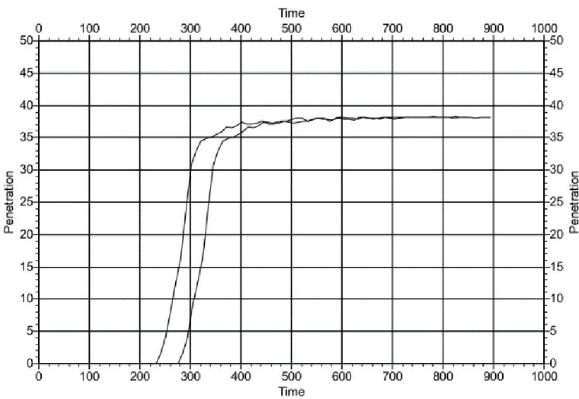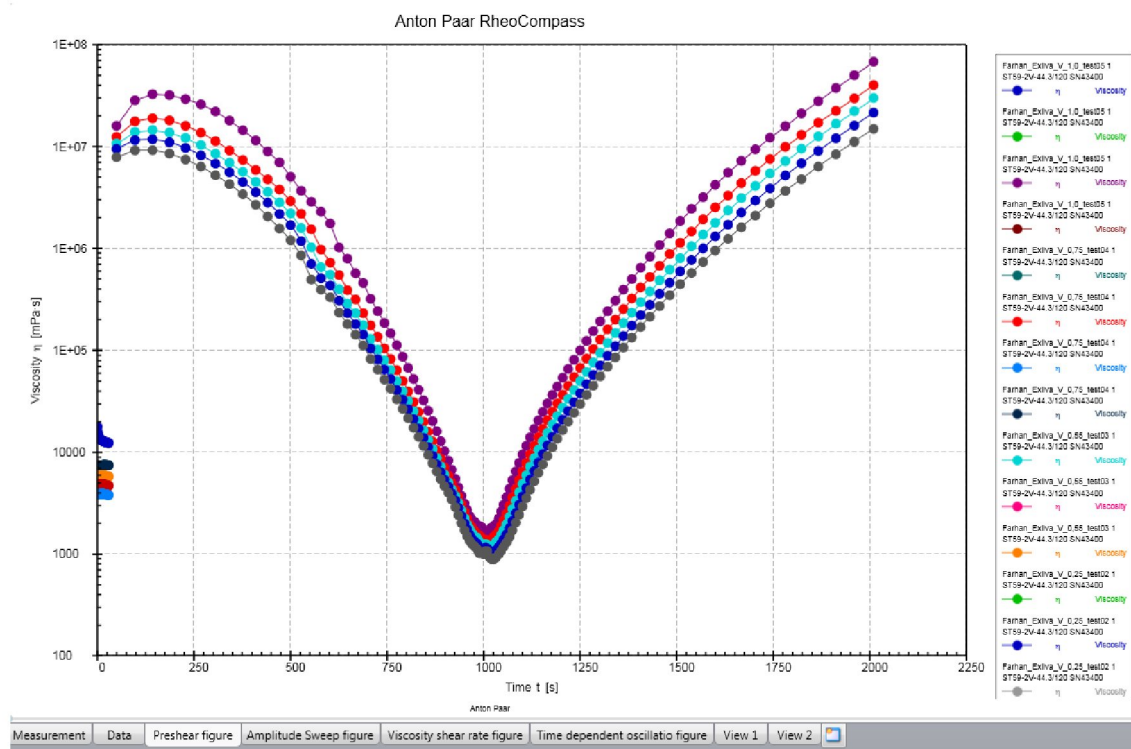CUSTOMER CODE : RC75   TIME TYPE   : FIXED
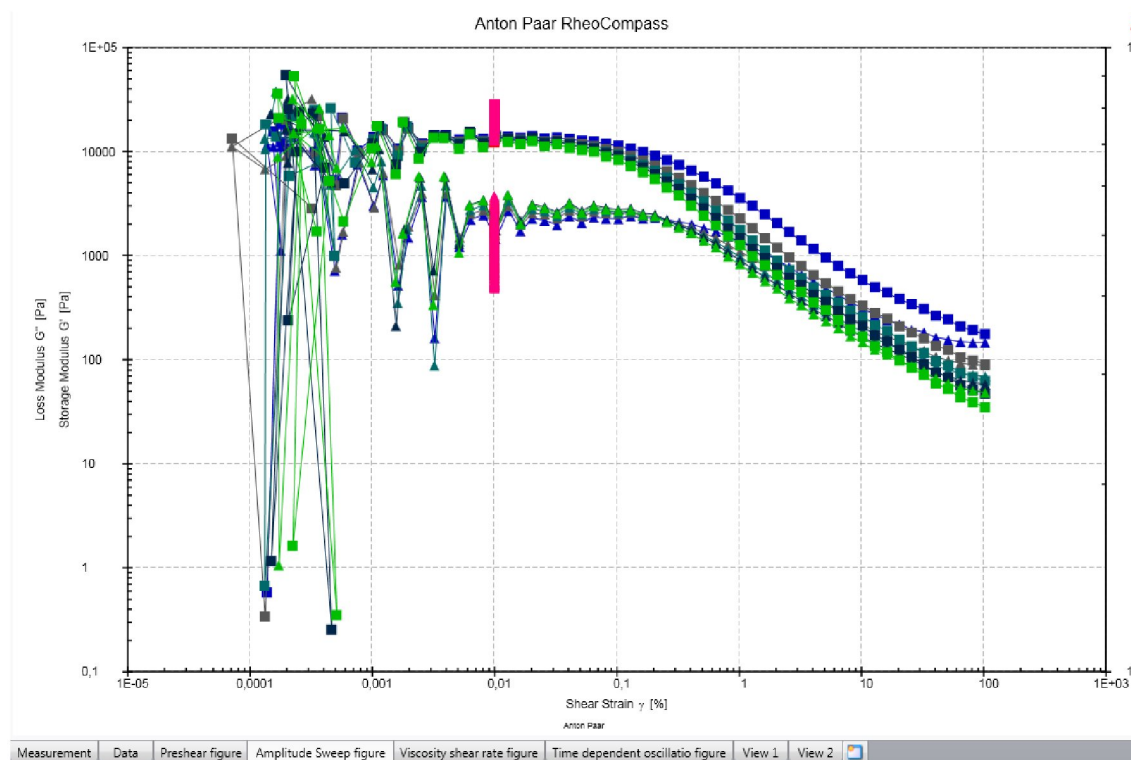
DATE OF TEST : 04/05/2023   FINAL SETTING : NO
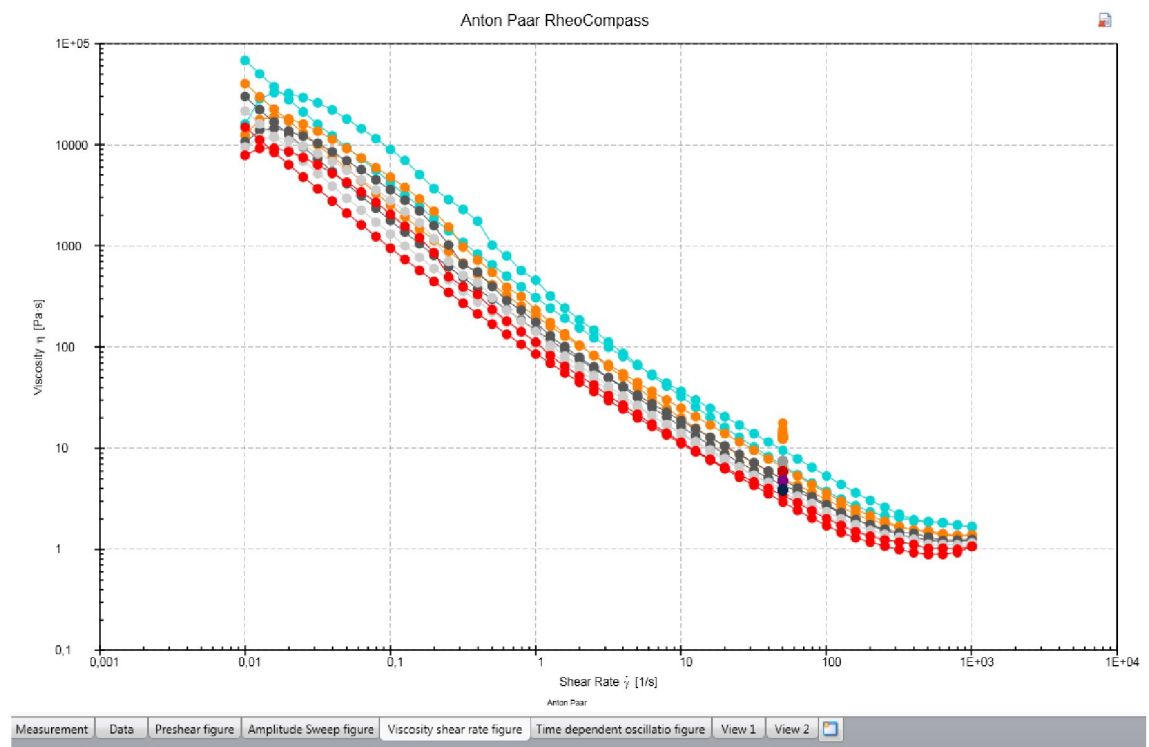
A.4.2. Rheological analysis
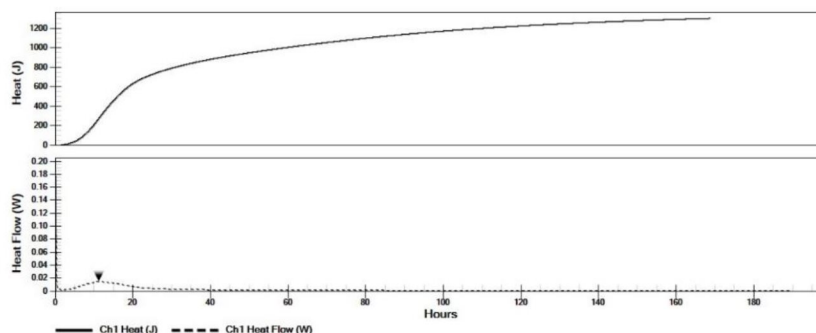
A.4.2.1   Pre-shear

A.4.2.1   Amplitude sweep

A.4.2.3.   Viscosity shear rate

A.4.3. Isothermal calorimetry

A.4.3.1. Control

Results	
Calorimeter Channel	1
Sample	
Sample ID	
Heat after 1 hour (J)	0.0098436
Heat after 1 day (J)	712.6
Heat after 3 days (J)	1065
Heat after 7 days (J)	1303.7
Time to peak (hr)	11.15
Peak max (W)	0.014802
Time to initial set point (hr)*	5.10
Time to final set point (hr)*	8.46

*Note: The time to initial and final set are approximate times that can be used for relative comparisons of different mixtures. The time to initial set is calculated as the time to reach 25% of the main hydration peak and the final set is calculated as the time to reach 75% of the main hydration peak. To be able to give more exact values for the setting times, the heat flow measurements need to be correlated with physical measurements.

Summary:
Channel: 1
Name: 1-control_23Mar
Start time: Mar 23, 2023 13:14:46
End time: Mar 31, 2023 11:12:54
Operator: FA
Results file path: C:\Users\farha\OneDrive - Østfold University College\Skrivebord\Calorimetry\Exilva
Sample:
Sample ID:
Total mass: 5.529

A.4.3.2.   MFC 0.1%
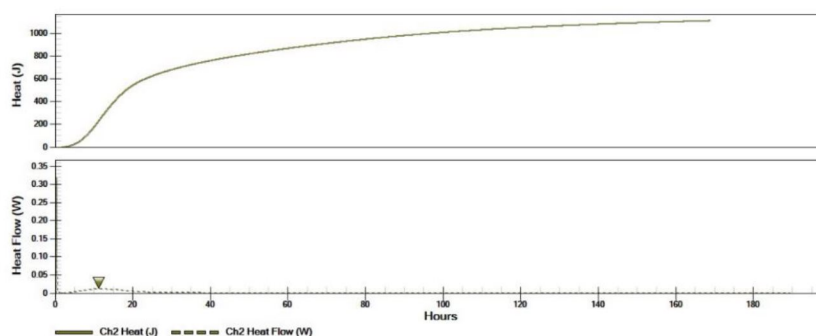
Results	
Calorimeter Channel	**2**
Sample	2-ExL-0_5_23Mar
Sample ID	
Heat after 1 hour (J)	0.0080051
Heat after 1 day (J)	616.65
Heat after 3 days (J)	924.43
Heat after 7 days (J)	1116.8
Time to peak (hr)	11.21
Peak max (W)	0.012884
Time to initial set point (hr)*	5.06
Time to final set point (hr)*	8.40

*Note: The time to initial and final set are approximate times that can be used for relative comparisons of different mixtures. The time to initial set is calculated as the time to reach 25% of the main hydration peak and the final set is calculated as the time to reach 75% of the main hydration peak. To be able to give more exact values for the setting times, the heat flow measurements need to be correlated with physical measurements.

Summary:
Channel: 2
Name: 1-ExL-0.1
Start time: Mar 23, 2023 13:17:02
End time: Mar 31, 2023 11:21:48
Operator: FA
Results file path: C:\Users\farha\OneDrive - Østfold University College\Skrivebord\Calorimetric analy
Sample: 2-ExL-0_5_23Mar
Sample ID:
Total mass: 4.737

A.4.3.2.   MFC 0.25%

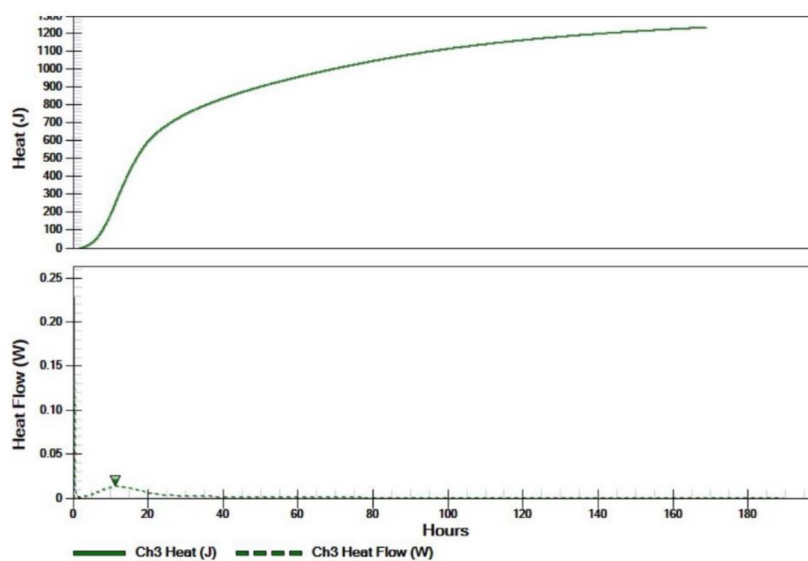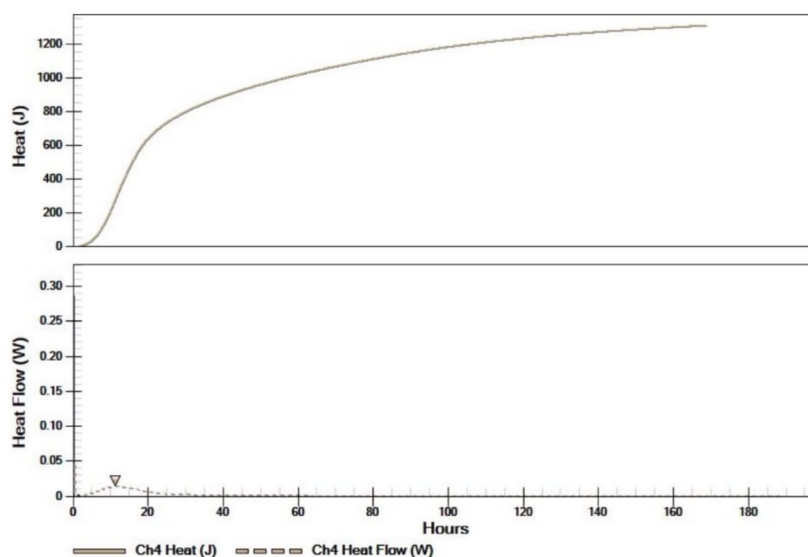| Results	
Calorimeter Channel	3
Sample	3-ExL-1_25-23Mar
Sample ID	
Heat after 1 hour (J)	0.008653
Heat after 1 day (J)	674.4
Heat after 3 days (J)	1014.3
Heat after 7 days (J)	1234.5
Time to peak (hr)	11.33
Peak max (W)	0.014099
Time to initial set point (hr)*	5.19
Time to final set point (hr)*	8.56

*Note: The time to initial and final set are approximate times that can be used for relative comparisons of different mixtures. The time to initial set is calculated as the time to reach 25% of the main hydration peak and the final set is calculated as the time to reach 75% of the main hydration peak. To be able to give more exact values for the setting times, the heat flow measurements need to be correlated with physical measurements.

Summary:
Channel: 3
Name: 2-ExL-0.25
Start time: Mar 23, 2023 13:18:52
End time: Mar 31, 2023 11:25:13
Operator: FA
Results file path: C:\Users\farha\OneDrive - Østfold University College\Skrivebord\Calorimetric analy
Sample: 3-ExL-1_25-23Mar
Sample ID:

A.4.3.2.   MFC 0.5%

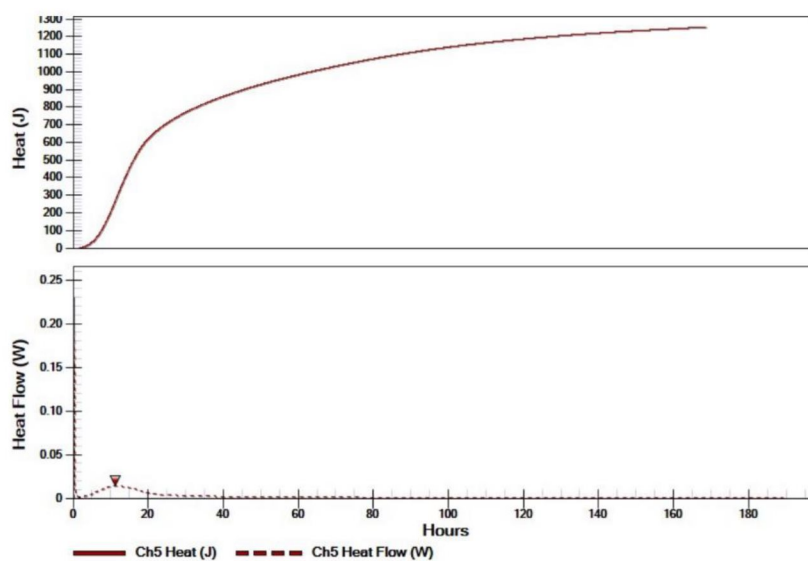| Results	
Calorimeter Channel	4
Sample	5.507
Sample ID	
Heat after 1 hour (J)	0.0098639
Heat after 1 day (J)	721.71
Heat after 3 days (J)	1079.3
Heat after 7 days (J)	1311.5
Time to peak (hr)	11.12
Peak max (W)	0.015059
Time to initial set point (hr)*	5.02
Time to final set point (hr)*	8.36

*Note: The time to initial and final set are approximate times that can be used for
relative comparisons of different mixtures. The time to initial set is calculated as the
time to reach 25% of the main hydration peak and the final set is calculated as the
time to reach 75% of the main hydration peak. To be able to give more exact values
for the setting times, the heat flow measurements need to be correlated with physical
measurements.

Summary:
Channel: 4
Name: 4-ExL-0.5
Start time: Mar 23, 2023 13:19:37
End time: Mar 31, 2023 11:28:15
Operator: FA
Results file path: C:\Users\farha\OneDrive - Østfold University College\Skrivebord\Calorimetric analy
Sample: 5.507
Sample ID:
Total mass: 5.507

A.4.3.2.   MFC 0.75%

Results	
Calorimeter Channel	5
Sample	5-ExL-3_75-23Mar
Sample ID	
Heat after 1 hour (J)	0.0090721
Heat after 1 day (J)	694.46
Heat after 3 days (J)	1041.9
Heat after 7 days (J)	1254.3
Time to peak (hr)	11.20
Peak max (W)	0.014715
Time to initial set point (hr)*	5.11
Time to final set point (hr)*	8.45

*Note: The time to initial and final set are approximate times that can be used for relative
comparisons of different mixtures. The time to initial set is calculated as the time to reach 25% of the
main hydration peak and the final set is calculated as the time to reach 75% of the main hydration
peak. To be able to give more exact values for the setting times, the heat flow measurements need to
be correlated with physical measurements.

Summary:
Channel: 5
Name: 5-ExL-0.75
Start time: Mar 23, 2023 13:20:10
End time: Mar 31, 2023 11:32:21
Operator: FA
Results file path: C:\Users\farha\OneDrive - Østfold University College\Skrivebord\Calorimetric analy
Sample: 5-ExL-3_75-23Mar
Sample ID:
Total mass: 5.39

A.4.3.2.   MFC 1.0%
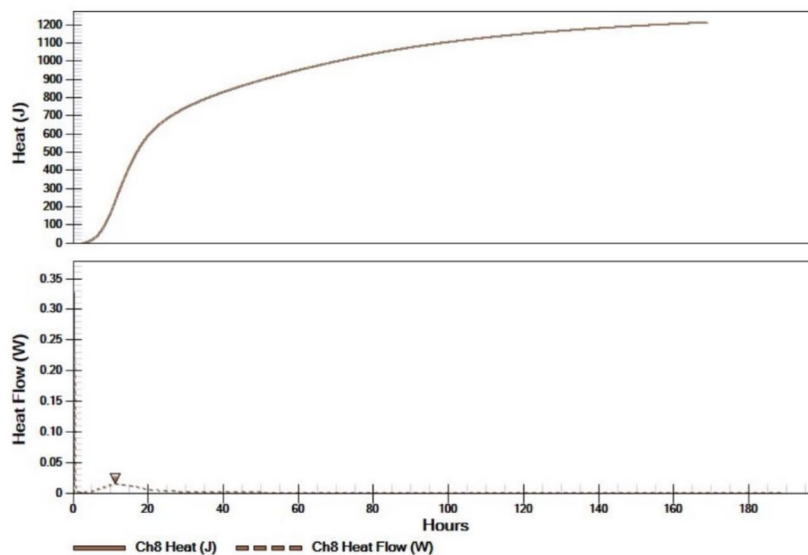
Results	
Calorimeter Channel	8
Sample	8-ExL-5--23Mar
Sample ID	
Heat after 1 hour (J)	0.0070414
Heat after 1 day (J)	673.22
Heat after 3 days (J)	1011.5
Heat after 7 days (J)	1216.9
Time to peak (hr)	11.28
Peak max (W)	0.015055
Time to initial set point (hr)*	5.76
Time to final set point (hr)*	9.03

*Note: The time to initial and final set are approximate times that can be used for relative comparisons of different mixtures. The time to initial set is calculated as the time to reach 25% of the main hydration peak and the final set is calculated as the time to reach 75% of the main hydration peak. To be able to give more exact values for the setting times, the heat flow measurements need to be correlated with physical measurements.

Summary:
Channel: 8
Name: 8-ExL-1.0
Start time: Mar 23, 2023 13:21:00
End time: Mar 31, 2023 11:36:46
Operator: FA
Results file path: C:\Users\farha\OneDrive - Østfold University College\Skrivebord\Calorimetric analy
Sample: 8-ExL-5--23Mar
Sample ID: